



# Fatigue Strength Assessment for Bulk Carrier According to Common Structural Rules

**Akram Madi**

**Master Thesis**

presented in partial fulfillment  
of the requirements for the double degree:  
"Advanced Master in Naval Architecture" conferred by University of Liege  
"Master of Sciences in Applied Mechanics, specialization in Hydrodynamics,  
Energetics and Propulsion" conferred by Ecole Centrale de Nantes

developed at West Pomeranian University of Technology, Szczecin  
in the framework of the

**"EMSHIP"**  
**Erasmus Mundus Master Course**  
**in "Integrated Advanced Ship Design"**

Ref. 159652-1-2009-1-BE-ERA MUNDUS-EMMC

Supervisor: Dr. Maciej Taczala, West Pomeranian University of  
Technology, Szczecin

Reviewer: Prof. Philippe Rigo, University of Liege

Szczecin, February 2012





## ABSTRACT

Structures of the bulk carriers are generally prone to fatigue due to high cyclic loads mainly caused by waves and changing loading conditions. During the past decades, a great number of fatigue failures occurred in ship structures, particularly in the areas built in higher tensile steel. Fatigue and corrosion are noted as predominant factors which contribute to the structural failure observed on a ship in service. Therefore, fatigue is an important criterion during design. The increasing demands placed on bulk carrier safety have reinforced the commitment of regulatory bodies to look for higher design standards and to improve the overall approach to design criteria. IACS has developed, for the first time, a unified complete set of Common Structural Rules for Bulk Carriers (CSR-BC). New CSR rules implement highly technical advanced methods to establish new criteria applied in a consistent manner. The problem of the fatigue strength is addressed in the present thesis where the hopper tank – inner bottom knuckle and longitudinal stiffener end connections being the structural details of 30,000 DWT double side skin bulk carrier are analyzed according to the IACS CSR-BC.

The fatigue assessment procedure within new CSR for bulk carriers are based on the following hypothesis: S-N curve approach, Palmgren-Miner's linear cumulative damage, dynamic fatigue load tuned on  $10^{-4}$  probability level in north Atlantic, design life 25 years, net scantling, load combination factors, fatigue loading conditions and Weibull probability distribution with two parameters for the long-term stress ranges load history.

Global finite element model followed by submodels according to IACS Rules for the corresponding locations is proposed to obtain the hot spot stresses for fatigue assessment. The primary mission is to develop a finite element model that can give the most accurate predictions of fatigue strength in the critical details for the relevant bulk carrier under CSR-BC with feasible computation and working efforts. GL-POSEIDON and ANSYS codes were used for the finite element analysis. POSEIDON provides specific tools for structural design, geometric and finite element modeling of bulk carriers under CSR-BC. ANSYS gives several options for fatigue analysis, post-processor and submodelling techniques. Critical review of design loads for fatigue assessment complying with relating to CSR-BC such as external and internal design pressure for different load conditions is accomplished and calculated using the Excel sheet. Coarse FEM model for the three midship cargo holds is created using four node shell element considering all loading conditions, full, alternate, normal ballast and heavy ballast and all load cases required by the Rules. Fine local FEM model of the hopper inner bottom knuckle and longitudinal stiffener web frame connection at midship cargo hold are built applying a four node shell element and fine mesh size  $t \times t$  where  $t$  is the inner bottom plate thickness. The displacement from global model is interpolated to the boundaries of local models. The fatigue hot spot stresses for hopper inner bottom knuckle are extrapolated based on the DNV recommendations for fatigue assessment. In addition, the geometry stress concentration factors for hopper inner bottom knuckle and longitudinal-web frame are estimated and compared with the IACS Rules values. The method of checking fatigue life for the relevant detail by Excel is also presented.

The result is shown that the corresponding total fatigue damage for the hopper inner bottom knuckle is less than the limit criteria of cumulative damage, and the detail has an acceptable fatigue life for 25 years operation in North Atlantic wave environment. The geometry stress concentration factor for that detail is higher than the simple estimation value calculated by CSR. The alternate loading condition has shown the highest stress range and elementary fatigue damage. In addition, the heavy ballast loading condition has high local mean stress and contributes significantly to the fatigue damage.

Key words: bulk carrier- IACS CSR-fatigue strength-hot spot stress-FEM-submodelling-ANSYS



## CONTENTS

ABSTRACT.....	3
1. INTRODUCTION.....	19
1.1. Background.....	19
1.2. Objectives and Work Scope.....	20
1.3. Assumptions for Fatigue Assessment.....	20
1.4. Methodology and Approach.....	21
1.5. Outlines of the Thesis.....	21
2. FATIGUE PRINCIPLES.....	23
2.1. Fatigue Assessment Overview.....	23
2.2. Fatigue S-N Curve.....	24
2.3. Fatigue Analysis Approaches.....	26
2.3.1 <i>Nominal Stress Approach</i> .....	26
2.3.2 <i>Hot Spot Approach</i> .....	27
2.4. Fatigue Damage.....	29
3. CSR FOR BULK CARRIERS.....	31
3.1. Introduction.....	31
3.2. Fatigue According to CSR.....	32
4. BULK CARTIER DESCRIPTION.....	35
4.1. General Specifications.....	35
4.2. Critical Areas against Fatigue.....	37
4.3. Load Calculation.....	38
4.3.1 <i>Ship Motions and Accelerations</i> .....	39
4.3.2 <i>Hull Girder Load</i> .....	41
4.3.3 <i>External Pressure</i> .....	41
4.3.4 <i>Internal Pressure and Loads</i> .....	42
5. GLOBAL FEM MODELING.....	45
5.1. Model Description.....	45
5.2. Material Model.....	48
5.3. Boundary Conditions.....	48
5.4. Load Analysis.....	49
5.5. Poseidon Model.....	50

5.5.1 Mesh Generation.....	53
5.6. ANSYS Model.....	56
6. SUBMODELLING.....	59
6.1. Hopper Inner Bottom Knuckle Submodel.....	60
6.2. Longitudinal Stiffener Web Frame Connection Submodel.....	63
7. RESULTS and ANALYSIS.....	65
7.1. Hot Spot Stress Extrapolation.....	65
7.2. Geometry Stress Concentration Factor.....	67
7.2.1 $K_g$ -Factor for Hopper Inner Bottom Knuckle.....	67
7.2.2 $K_g$ -Factor for Longitudinal Stiffener Web Frame Connection.....	70
7.3. Cumulative Fatigue Damage for Hopper Inner Bottom Knuckle.....	74
8. CONCLUSIONS AND RECOMMENDATIONS.....	79
9. ACKNOWLEDGEMENTS.....	81
10. REFERENCES.....	83
APPENDICES.....	85

## LIST OF FIGURES

Figure 2-1: S-N curve.....	25
Figure 2-2: Types of stresses.....	28
Figure 2-3: Miner summation procedure for one stress block.....	30
Figure 3-1: Flowchart of direct FEM fatigue assessment.....	33
Figure 4-1 (a): Midship section of DSS bulk carrier.....	36
Figure 4-1(b): DSS bulk carrier.....	36
Figure 4-2: Fatigue crack locations and orientation in typical bulk carrier.....	38
Figure 4-3: Ship accelerations.....	40
Figure 4-4: Distribution of hydrodynamic pressure $p_1$ at midship.....	42
Figure 4-5: Double skin bulk carrier.....	43
Figure 5-1: Half section in the geometry of global model.....	46
Figure 5-2: Midship web frame section.....	47
Figure 5-3: View of cargo hold No. 4 structural elements.....	47
Figure 5-4: Cargo hold No. 4 compartment model.....	50
Figure 5-5: General arrangement of midship.....	51
Figure 5-6: Configuration of ballast/fuel tanks content.....	51
Figure 5-7: Configuration of cargo hold loading for fatigue assessment.....	52
Figure 5-8: Shell quad and triangle elements.....	53
Figure 5-9: First model with shell element for plate and beam element for stiffener.....	54
Figure 5-10: Second model-view of inner bottom stiffener mesh.....	55
Figure 5-11: Boundary at end plane.....	56
Figure 5-12: Von Mises stress in full load condition (sagging heading sea case).....	57
Figure 6-1: Hopper inner bottom knuckle geometry.....	60
Figure 6-2: Hopper inner bottom knuckle mesh.....	60
Figure 6-3: Hopper inner bottom model cut boundaries.....	61
Figure 6-4: Displacement interpolation from global model to local model.....	61
Figure 6-5: First principal stress in fine and coarse model.....	62
Figure 6-6: Longitudinal-web frame connection model.....	63
Figure 6-7: Longitudinal-web frame local model mesh.....	63
Figure 6-8: Longitudinal stiffener web frame model cut boundaries.....	64

Figure 6-9: Third principal stress distribution in longitudinal-web frame local model.....	64
Figure 7-1: Hot spot stress extrapolation.....	65
Figure 7-2: Hot spot at hopper Inner bottom knuckle.....	66
Figure 7-3: Vectors of principal stresses at element nodes.....	66
Figure 7-4: First principal element midpoint stress .....	68
Figure 7-5: First principal stress at nodes.....	68
Figure 7-6: First principal stress at nodes from coarse model.....	69
Figure 7-7: Third principal stress distribution in longitudinal-web frame local model.....	70
Figure 7-8: Detail in double bottom.....	71
Figure 7-9: Element stress for longitudinal-web frame connection.....	71
Figure 7-10: Element center point principal stress in longitudinal-web frame model.....	72
Figure 7-11: Path of hot spot stress for longitudinal-web frame local model.....	72
Figure 7-12: Element stress distribution in longitudinal-web frame from global model.....	73
Figure 7-13: Elementary and cumulative fatigue damage for hopper inner bottom knuckle...77	



## LIST OF TABLES

Table 4-1: Bulk carrier principle specifications.....	35
Table 4-2: Members and locations subjected to fatigue strength assessment.....	37
Table 4-3: Bulk carrier motions and accelerations.....	40
Table 4-4: Hull girder loads.....	41
Table 4-5: Total external pressure at full loading condition.....	42
Table 4-6: Inertia and still water pressure due cargo in hold No. 4.....	43
Table 5-1: Material properties.....	48
Table 5-2: Rigid-link of both ends .....	48
Table 5-3: Support condition of the independent point.....	48
Table 5-4: End section boundary condition.....	49
Table 5-5: Definition of load cases.....	49
Table 5-6: Cargo holds/tanks volume.....	50
Table 5-7: Maximum loading in cargo hold.....	52
Table 7-1: Hot spot stress and loading ‘condition 1’.....	75
Table 7-2: Equivalent notch stress range.....	76
Table 7-3: Elementary Fatigue damage for hopper inner bottom knuckle.....	77



## List of Appendices

Appendix A1: Load Combination Factors.....	85
Appendix A2: Standard Loading Condition for Fatigue Assessment.....	86
Appendix A3: Deformation in Global Coarse Model (Poseidon Code).....	87
Appendix A4: Principal Stress in Coarse Model and Submodel for Homogenous Loading Condition.....	88
Appendix A5: Principal Stress in Coarse Model and Submodel for Alternate Loading Condition.....	89
Appendix A6: Principal Stress in Coarse Model and Submodel for Normal Ballast Loading Condition.....	90
Appendix A7: Principal Stress in Coarse Model and Submodel Heavy Ballast Loading Condition.....	91
Appendix A8: Principal Stress in Coarse Model Homogenous and Alternate Load .....	92
Appendix A9: Midship Section of DSS Bulk Carrier (Poseidon Code).....	93
Appendix A10: Ordinary Frame Midship Section in Cargo Hold.....	94
Appendix A11: Path of nodal principal stress for different loading conditions from hot spot.	95



## NOMENCLATURE

$\Delta S$	Stress range
$N$	Number of Cycle
$\sigma_n$	Nominal stress
$F$	Force
$A$	Area
$M$	Moment
$W$	Section modulus
$D$	Cumulative fatigue damage
$K_g$	Geometry stress concentration factor
$K_w$	Notch stress concentration factor
$t$	Thickness
$\sigma_g$	Geometry hot spot stress
$T_{LC}$	Scantling draught at full load condition
$M_{WV,H}$	Wave vertical bending moment hogging
$M_{WV,S}$	Wave vertical bending moment sagging
$M_{SW,H}$	Still water vertical bending moment hogging
$M_{SW,S}$	Still water vertical bending moment sagging
$M_{W,H}$	Wave horizontal bending moment
$Q_{WV}$	Wave vertical shear force
$R_{eH}$	Minimum yield stress
$\zeta$	Weibull shape parameter
$\Gamma$	Upper case non-normalize incomplete gamma function
$\gamma$	Lower case non-normalize incomplete gamma function
$\Delta\sigma_{eq}$	Equivalent notch stress range
$\Delta\sigma_{equiv}$	Equivalent hot spot stress range
$\sigma_{mean}$	Structural hot spot mean stress
$\Delta\sigma_W$	Hot spot stress range



## ABBREVIATION

IACS	International Association of Classification Society
CSR-BC	Common Structural Rules for Bulk Carriers
BV	Bureau Veritas
DNV	Det Norske Veritas
GL	Germanischer Lloyd
LR	Lloyd's Register
KR	Korean Register
ABS	American Bureau of Shipping
SSC	Ship Structure Committee
FEM	Finite Element Method
DSS	Double Side Skin
HSE	Health and Safety Executive
IIW	International Institute of Welding
DSA	Direct Scantling Assessment
SCF	Stress concentration factor





***Declaration of Authorship***

*I declare that this thesis and the work presented in it are my own and have been generated by me as the result of my own original research.*

*Where I have consulted the published work of others, this is always clearly attributed.*

*Where I have quoted from the work of others, the source is always given. With the exception of such quotations, this thesis is entirely my own work.*

*I have acknowledged all main sources of help.*

*Where the thesis is based on work done by myself jointly with others, I have made clear exactly what was done by others and what I have contributed myself.*

*This thesis contains no material that has been submitted previously, in whole or in part, for the award of any other academic degree or diploma.*

*I cede copyright of the thesis in favour of the University of West Pomeranian Technology, Szczecin.*

*Date:*  
15-01-2012

*Signature*

A handwritten signature in black ink, consisting of a stylized initial 'A' followed by a series of horizontal and vertical strokes.



## **1. INTRODUCTION**

### **1.1. Background**

During the past years, a great number of fatigue failures occurred in ship structures, especially in areas constructed with higher tensile steel. Fatigue and corrosion are recognized as predominant factors which contribute to the structural failure observed on a ship in service. In the early 1990s, following the occurrence of cracks in side shell longitudinal of very large crude carriers after only a few in service, all major classification societies issued or revised rules and guidelines for explicit fatigue analysis.

The increasing demands placed on Bulk Carrier safety have reinforced the commitment of regulatory bodies to look for higher design standards and to improve the overall approach to design criteria. IACS has developed, for the first time, a unified complete set of Common Structural Rules for Bulk Carriers. New CSR rules implement advanced structural and hydrodynamic computational methods to establish new criteria applied in a consistent manner, which will result not only in a more robust, safer ship, but will also eliminate the possibility of using scantlings and steel weight as a competitive element when selecting a class society to approve a new design.

Ship structures are exposed to different types of loads during voyages. The loads include wave- induced dynamic load, hydrostatic load, transient impact/slamming load, sloshing load, thermal load and so on. Fatigue may be defined as a process of cycle by cycle accumulating of damage in a structure subjected to fluctuating stresses.

The aim of the fatigue assessment is to ensure that all parts of the hull structure subjected to dynamic loading have an adequate fatigue life. To ensure that the structure will fulfill its intended function, a fatigue assessment should be carried out for each individual type of structural detail that is subjected to extensive dynamic loading.

## 1.2. Objectives and Work Scope

The overall objective of proposed work is to assess the fatigue strength of primary members and stiffeners of bulk carrier according to Common Structural Rules for Bulk Carriers. That will help the designers and classification societies to verifying the new Common Structural Rules. In achieving the main objective the following secondary objectives is to be considered:

- Develop finite element models (FEM) according to the requirement of Common Structural Rules (CSR) for bulk carriers.
- Develop submodels for evaluating the stress concentration factor (SCF) and compare the results with CSR-tabularized values.
- Assess the fatigue strength according to the CSR.

## 1.3. Assumptions for Fatigue Assessment

In recent years Classification Societies, have introduced fatigue assessment requirements in order to improve the fatigue life of critical details by providing attention to construction details at the design stage. The new Rules include a mandatory set of requirements for fatigue assessment of all construction details currently covered within the classification requirements of ABS, DNV and Lloyd's Register. The fatigue assessment procedure within the New Rules is based on the following principle assumptions:

- S-N curve approach for the fatigue strength capacity.
- Use of cyclic stresses derived from the application of the different kinds of specified loads (the effect of mean stress is includes).
- Design fatigue life of the vessel equal to 25 years.
- Long-term stress ranges load history of each structural detail represented by two-parameters of Weibull probability distribution.
- Long-term environmental data relevant to the North-Atlantic Ocean (based on the IACS Wave Data).
- Linear cumulative damage model based on the Palmgren-Miner's summation method.

## 1.4. Methodology and Approach

The objectives of the study will be achieved by the following approaches:

- Study deeply and extensively literature related to fatigue assessment approach's for ship structures.
- Review the new Common Structural Rules for bulk carriers and study the historic development for that rules.
- Collect the data for the relevant bulk carrier ship.
- Develop global finite element model under CSR requirement. Finite element analyses were performed in order to check the stress distribution and deformations in the model and to evaluate the local stresses at critical hot-spots, i.e. structural hot-spots stresses.
- Develop local models for the selected critical details primary member and stiffener. The local models were used as submodels to the global analysis. From submodel analysis, the local hot spot stress due to geometry is determined using element size in the order of plate thickness for fatigue damage calculation and to pick up the geometry stress concentration factor.
- Evaluate the fatigue strength according to IACS rules for bulk carriers and analyze the results.

## 1.5. Outlines of the Thesis

This thesis is organized as follow:

*Chapter one*, gives brief introduction on the problem, assumptions and the work done in that thesis.

*Chapter two*, a general theoretical basic and principles for fatigue is introduced. It is more focus on the fatigue approaches especially on the nominal and hot spot stress approaches.

*Chapter three*, short description on the common structural rules for bulk carriers with presenting the new design key element for that rules and flowchart for fatigue assessment according to IACS rules.

*Chapter four*, present the characteristic specifications for the relevant Handysize double side skin bulk carrier that selected for fatigue assessment with focusing on the critical areas and considering loads for fatigue strength calculation.

*Chapter five*, a global finite element model for three midship cargo holds based on CSR-BC was developed for fatigue assessment using Poseidon FEM code for bulk carriers. In addition, the FEM model has been transferred to ANSYS software for the post-processing.

*Chapter six*, describe the submodelling techniques using the interpolated displacement method from global coarse model to the cut boundary of submodel. In addition, two submodels for hopper inner bottom knuckle and longitudinal stiffener web frame connection, at midship cargo hold No. 4 for fatigue analysis are created and checked.

*Chapter seven*, present results and discussions for hopper inner bottom knuckle and longitudinal-web frame end connection members.

*Chapters eight*, illustrate the final conclusions and recommendations for that piece of work.

## 2. FATIGUE PRINCIPLES

### 2.1. Fatigue Assessment Overview

Yingguang (2010) noted that the fatigue assessment technique can be categorized as following: the “Simplified method”, the “spectral-based method” and the “deterministic method”. The “Simplified fatigue assessment method”, the long-term stress range distribution of a ship structural element is assumed to follow the Weibull probability distribution. While this is a simplified fatigue assessment technique, some engineering judgment is still required in applying the method to actual design (e.g., in deciding the Weibull shape parameter and in choosing basic design S-N curves).

The “Spectral-based fatigue analysis” is a direct calculation method. In the spectral approach, various orders of spectral moments of the stress process are obtained by performing a first principle based Seakeeping analysis (i.e. finding the motions and related quantities of a vessel subjected to a sea state) and sub-sequent mathematical manipulations. Using the spectral moments, the Rayleigh probability density function describing the short-term stress range distribution, the zero-up crossing frequency of the stress response and the spectral bandwidth parameter used in calculating the cycle counting correction factor for a wide band random process are then calculated. The total fatigue damage of a structural element is calculated by adding up the short-term damages over all the applicable sea states in specific wave scatter diagram. Therefore, the spectral method can account for various sea state as well as their profanities of occurrence.

The “Deterministic method” may be considered as a “Simplified” version of the spectral method. The main simplification involves how wave-induced load effects are characterized. In the spectral approach, short-term wave spectral formulations (such as the Pierson-Moskowitz wave elevation spectrum) are used to characterize the expected energy in individual sea states. In the deterministic approach, a sea state is simply characterized by using a deterministic wave height and period. Sound engineering judgment based on the designers’ practical experience is needed in order to properly select the collection of the deterministic waves that will be sufficient to establish the fatigue demand that the structure element will experience.

Sharp (1993) gives data for the uncertainties in prediction of fatigue life for North Sea platforms. The main uncertainties in estimation of fatigue life are in the SN-curve and the stress concentration factor (SCF) used.

Lotsberg (2006a and 2007) presented a fatigue assessment method based on FEA, where a link between calculated hot spot stress and fatigue capacity was established. The papers give a review of the fatigue calculations using finite element analysis and provide recommendations to perform fatigue assessment of plated structures based on finite element analysis combined with one hot spot S-N curve.

Fatigue design methods for ship and offshore structures are discussed in ISSC (2009), for ships, rule-based-methods for fatigue evaluation are proposed by classification societies, and a comparison of the different fatigue methodologies provided by BV, DNV, GL, KR, LR and NK are summarised.

## 2.2. Fatigue S-N Curve

The S-N curve as seen in Figure 2-1 expresses the number of cycles to failure  $N$  by the stress range  $S$  for constant amplitude (stress range) loading. It is determined empirically by laboratory fatigue testing, for various geometries of welded structures details. S-N curve gives the relationship between the nominal stress ranges  $S$  applied to a given sample and the number of load cycles  $N$  to failure:

$$(\Delta S)^m \cdot N = C \quad (2-1)$$

Where  $m$  and  $C$  are constant depend on material and weld type, type of loading, geometrical configuration and environmental conditions.



Fatigue strength assessment of a bulk carrier  
according to Common Structural Rules

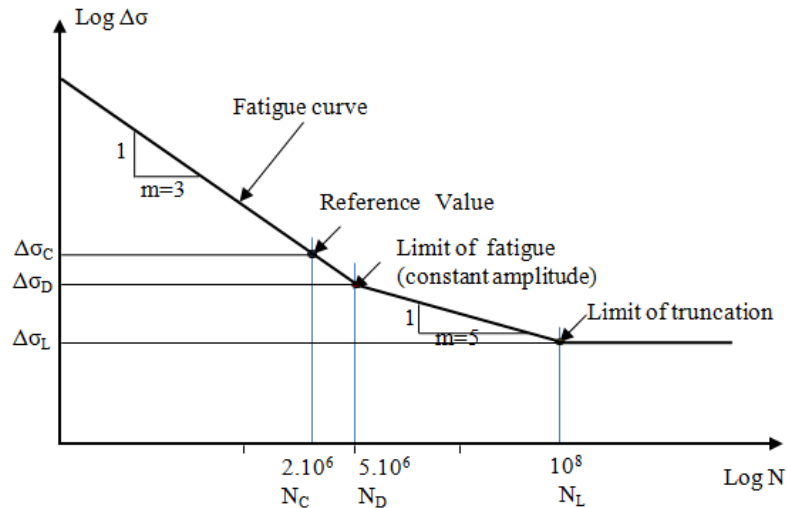


Figure 2-1: S-N curve

Design S-N curves are based on constant amplitude fatigue tests of in general small scale specimen. A statistical analysis is to be performed to determine the mean regression line on a log-log scale. Confidence intervals based on the standard deviations of the test results will be within the given limit. Most design S-N curves are based on the mean minus two standard deviation curves for relevant experimental data. They are thus associated with a 97.6% probability of survival.

For fatigue design of structural details several engineering guidelines have been established. The fatigue strength in these guidelines is normally characterized by a set of empirical S-N curves for different weld details. The international Associations of Classification Societies (IACS) recommends two sets of S-N curves to be used for assessment of the fatigue strength of structural details:

- HSE (Health and Safety Executive) Basic S-N Curves.
- IIW (The International Institute of Welding) S-N Curves.

HSE set has eight curves, each changes slope at  $10^7$  cycles and each curve represents a class of welded details. The IIW has established 14 curves for various welded structural details. Slope change for each IIW curve is at  $N = 5 \cdot 10^6$ . Both sets of curves are well known and described in details (IACS, 1999).

The S-N curves are generally determined in laboratories, which needs some modifications to basic S-N curves, keeping in mind that these curves will be used to assess the fatigue strength of actual structures. A number of factors should be considered:

- Corrosion
- Plate thickness
- Weld improvement
- Residual stresses
- Mean stresses
- Workmanship

The appropriate SN curve must be selected in the fatigue assessment procedure according to the stress approach applied. Traditionally fatigue calculations were based on the nominal stresses and the use of geometry dependent S-N curves. If for a particular detail the S-N curve is specifically tested, then the nominal stress approach can be quite accurate. Unfortunately a large number of ship structural details are different from the details the traditional S-N curves have been derived for. Thus, how to choose appropriate S-N curve can be quite a difficult task when using nominal stress approach.

### **2.3. Fatigue Analysis Approaches**

There are different approaches to fatigue life prediction. These approaches have different in the extent of stress and strain analyses, i.e. the levels of stress risers, which are taken into account. Four basic approaches has been exit as following:

- The nominal stress approach
- The hot spot stress approach
- The notch stress / strain approach
- The fracture mechanics approach

This paper of work will describe the first three approaches.

#### ***2.3.1 Nominal Stress Approach***

The nominal stress approach is based on far-field stresses due to forces and moments at the potential site of cracking or the stresses not containing any stress increase due to structural details or welds. Moreover, the nominal stress  $\sigma_n$  can be defined as the stress which is derived from beam theory or from coarse mesh FEM models based on the applied loads and dimensions of the component. Increase in stresses due to discontinuities in structural geometry and presence of welds is disregarded when calculating nominal stresses.

Nominal stress is generally calculated in simple component by resolving to general theories (e.g., the beam theory) based on linear-elastic behavior, for more complex structures, if no analytical solutions are available, it may be calculated resorting to simple and coarse FE mesh models.

$$\sigma_n = F/A + M/W \quad (2-2)$$

The nominal stress approach forms the basis for most design rules for steel structures and therefore widely used. Nominal stress yields satisfactory results with minimum calculation effort under the following conditions:

- There is well defined nominal stress, not complicated by global geometric effects.
- The local geometry is comparable with one of those compiled in the design classifications rules.
- Variable amplitude loading is not consisting mainly of stress ranges below the constant amplitude endurance limit.

The fatigue strength is defined through S-N curves. The S-N curves used in combination with nominal stresses are determined by testing either small specimen or near full-scale beams. It is essential that stress used to develop the S-N curves is the nominal stress. The local geometry effect and the local notch effect are thus implicitly included in the denoted fatigue strength.

### **2.3.2 Hot Spot Approach**

The structural or hot-spot stress approach, in other words also called geometric stress approach, considers the stress increase due to the structural configuration or the macro-geometry. A hot spot is critical point in a structure, usually at weld toe where a fatigue crack is supposed to initiate. The hot spot stress as shown in Figure 2-2 is the value of structural stress at the hot spot position. Furthermore, the hot spot is located at a local notch where the peak stress caused by local notch is excluded from the hot spot stress.

The structural stress can be defined as the summation of membrane and shell bending stresses in structures consisting of plate elements or curved shells. The structural stress can be calculated by any suitable method, e.g. by theory of shells or the finite element method (FEM). The structural stress contains the effects of geometric discontinuities which can be caused e.g. by welded attachment or misalignment.

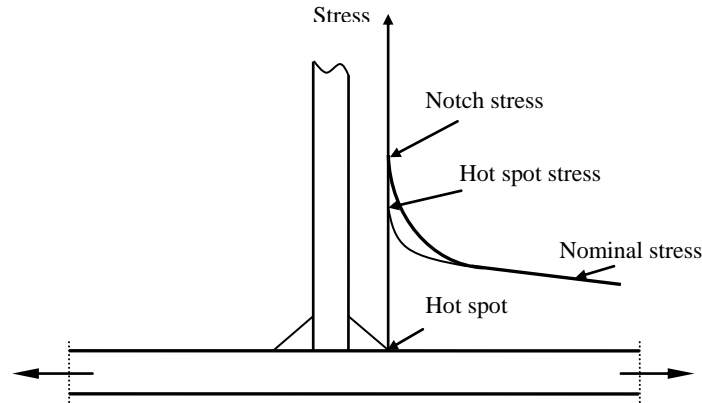


Figure 2-2: Types of stresses

IIW define the hot spot stress as following, the hot spot is determined by extrapolating principle stress to the weld toe where the extrapolated principle stress has its maximum value. The extrapolation must be carried out from the region outside the influence of the effects of the geometry and discontinuities at the weld toe, but close enough to fall inside the zone of the stress gradient caused by the global geometrical effects.

There are three possible ways to determine the hot spot stress for a welded detail.

- By computing the nominal stress and multiplying it by the stress concentration factor which valid for the local geometry.
- By FEM using shell or solid elements and carrying stress analysis.
- By experimental model test at hot spot.

One advantage of hot spot approach is that one S-N curve can be used to predict the fatigue life of many types of joint configurations. Different S-N curves are only needed if the variation in the smoothness of the local notch or the material thickness effect is taken into account.

### ***2.3.3 Notch Stress/ Strain Approach***

The notch stress approach is based on the stress / strain state at the notch directly, taking into account all stress raisers, including the local stress peak due to the geometry of the notch itself. The approach has its foundations in the so-called notch root approach, which is valid for notched members in general. The notch stress approach has received much attention lately due to the increasing available computational power and the need for assessing more increasingly complex geometries.

Only one S-N curve is required for all details in the notch stress approach. Stress concentrations due to structural geometry and weld are considered in the stress calculation. Disadvantage of this approach is that it may be difficult to describe the geometry of the local notch at a weld.

## 2.4. Fatigue Damage

Fatigue failure can be proceed in three distinct stages: crack initiation in the areas of stress concentration (near stress raisers), incremental crack propagation, and final catastrophic failure. Applied stress causing fatigue may be axial (tension or compression), flexural (bending) or torsional (twisting). The development of fatigue cracks due to cyclic loading is a phenomenon common to many engineering applications. It can be observed and is of particular concern in ships, bridges, pressure vessels, aircraft and offshore installations. The consequence of fatigue failure can range from simple nuisance cracks that are mainly a concern of maintenance and inspection to complete structural failure resulting in the loss of lives and property. The accurate estimation of fatigue endurance is therefore of great importance for both design and maintenance purposes.

The fatigue life of a given structural component depends on several influencing factors:

- **Long-term cyclic loading:** since fatigue damage is a cumulative process the distribution of the cyclic stress components is the most important factor that determines the fatigue life. In general the long-term load distribution has to be described on a statistical basis and depend on the type of structure and the operating environment.
- **Material properties:** different materials have in general different fatigue strength properties, which have to be determined experimentally.
- **Local stress concentration:** the process of local stress concentrations caused by a specific detail geometry or construction flaws such as misalignment magnifies the cyclic stress component and thus reduces the fatigue life.
- **Construction method:** construction characteristics can greatly reduce the fatigue strength of structural detail. The presence of welds in steel structures is the main cause of fatigue failures.

The fatigue life of structural detail can be calculated using the theory of cumulative damage. Cumulative damage is in general the fatigue damage under stochastic or random loading. The most will be known theory to calculate the cumulative damage is the Palmgren-Miner

summation model as shown in Figure 2-3. The basic assumptions in the Miner summation method is that the damage  $D$  for one load cycle is:

$$D = \frac{1}{N} \quad (2-3)$$

Where  $N$  defines the number of constant amplitude cycles at a given stress range that cause failure. For a long term load on structure consisting of  $i$  blocks of stress ranges  $S_{r_i}$  each with a number of cycles  $n_i$ , the cumulative damage can be obtained by the following equation:

$$D = \sum_{i=1}^k \frac{n_i}{N_i} \quad (2-4)$$

Failure occurs when  $D=1$ ,  $N_i$  defines the number of cycles to failure for the stress range in block  $i$ .

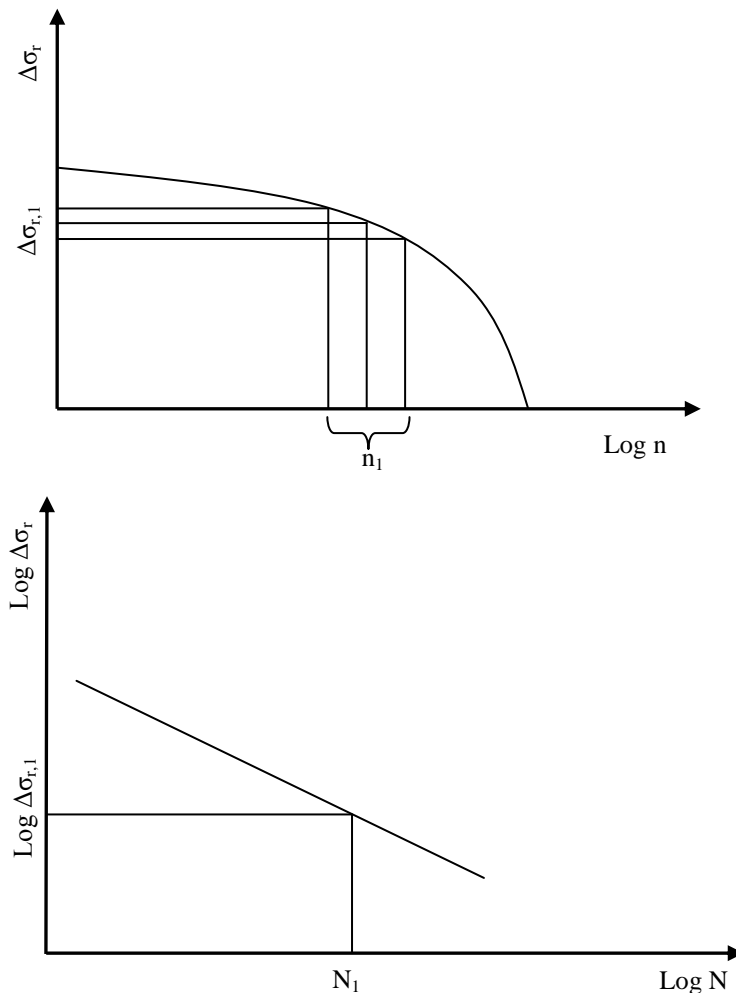


Figure 2-3: Miner summation procedure for one stress block

### 3. CSR FOR BULK CARRIERS

#### 3.1 Introduction

The Common Structural Rules for Bulk Carriers (CSR-BC) have been developed to help the classification societies by creating one single set of rules to be applied uniformly by all International Association of Classification Societies (IACS) members. The great aim is to provide a standard that can help engineers to apply appropriate design, with a suitable distribution of structural scantlings to withstand the loads likely to be encountered during the ship's operational lifetime and with corrosion margins based on the collective experience of the industry.

The IACS CSR-BC entered into force on 1<sup>st</sup> April 2006, and applies to all bulk carriers with length above 90 meters and all double oil tankers with length above 150 meters. The background and basis for common structural rules development has been discussed by Lovstad et al. (2007), and Horn and Baumans (2007) outlined challenges in rule development regarding modeling technique, structural response and acceptance criteria.

Since April 2006, few amendments to the CSR were made in an effort to harmonies the CSR for tankers and bulk carriers, and the latest versions of the rules were published on July 2010. IACS also published common interpretations for the rules to assist its member societies and industry in implementing the CSR in a uniform and consistent manner. There is also long-term plan put in place to further increase harmonization between the tanker and bulk carrier common structural rules. The key elements of the Common Structural Rules for bulk carriers include:

***Design Life:*** Design criteria target a design life of 25 years for the ship in the North Atlantic environment. The actual service life will depend upon the vessel's operational profile and maintenance.

***Net Thickness:*** The Common Structural Rules adopt the net thickness approach to scantlings. This provides a direct link between the thickness that is used for strength calculations during the design stage and the minimum steel thickness acceptable during the operational life of the ship. The strength calculations are based on the net scantling approach. Newbuilding gross

scantling requirements are calculated by the addition of an allowance for the expected wastage during the design life of the vessel.

**CSR Direct Scantling Assessment (DSA):** For bulk carriers with a length of 150 m and greater, the new Rules require a mandatory finite element analysis of the midship cargo block, extending over three holds (DSA is not required for CSR bulk carriers of less than 150 m).

**CSR Fatigue Assessment:** The new Common Rules include a mandatory set of requirements for fatigue assessment using the 25-year North Atlantic design life.

**CSR Buckling:** Buckling is also specifically addressed. The Rules have two levels of buckling check, based on prescriptive formulations initially and a buckling check based on finite element analysis.

### **3.2 Fatigue according to CSR**

Fatigues according to IACS rules for bulk carriers depend on the following principles; the minimum design life 25 years in North Atlantic environment, classic Palmgren-Miner cumulative rule, long term stress distribution, dynamic fatigue loads tuned on  $10^{-4}$  probability level (North Atlantic), load combination factors, fatigue loading conditions (homogenous, alternate, normal ballast and heavy ballast), static load also included and net scantling. The procedures to evaluate the fatigue strength by direct FEM analysis are seen in Figure 3-1.



Fatigue strength assessment of a bulk carrier  
according to Common Structural Rules

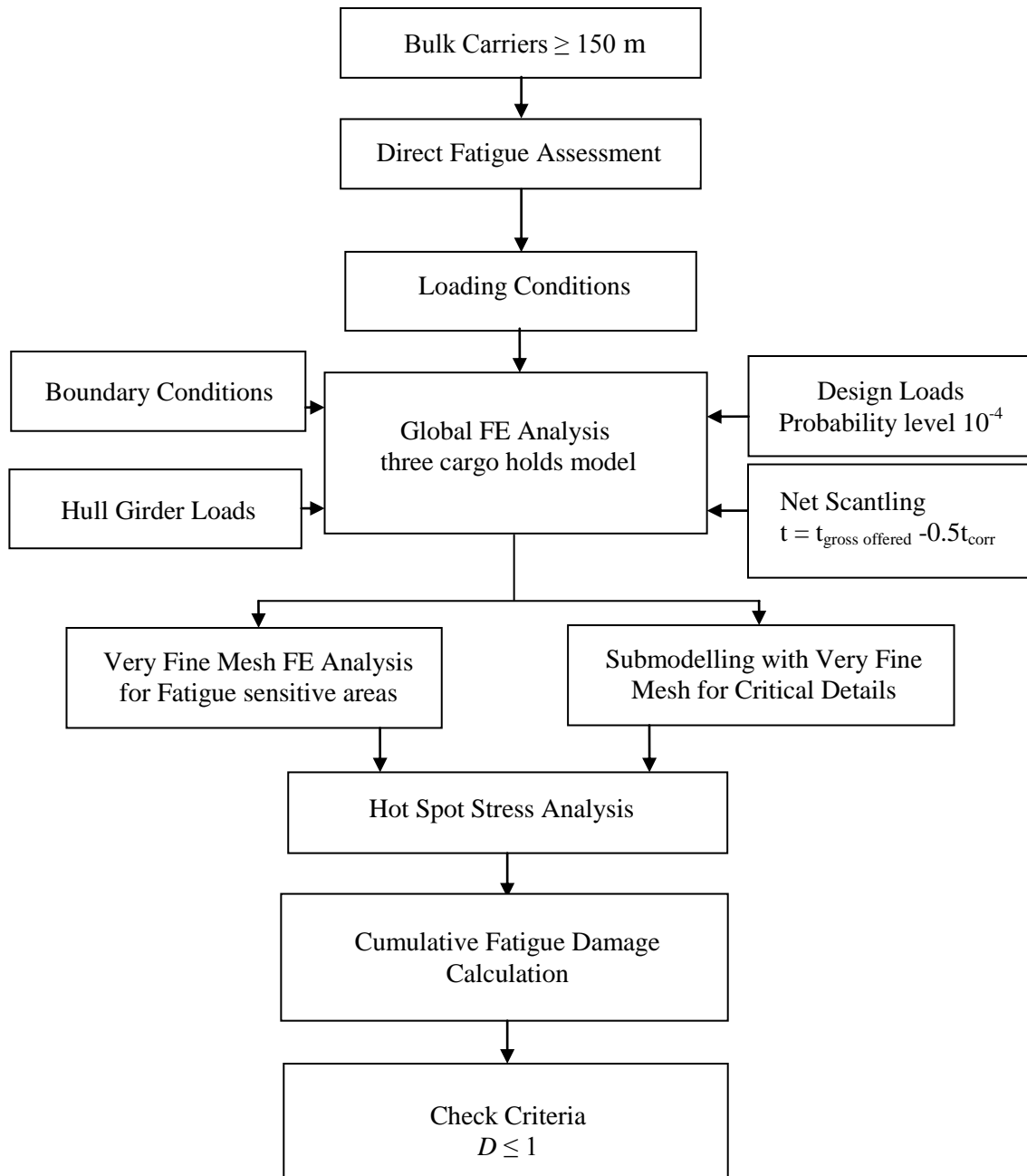


Figure 3-1: Flowchart of direct FEM fatigue assessment



## 4. BULK CARRIER DESCRIPTIONS

Bulk Carriers, defined as ships constructed with topside tanks and hopper side tanks in cargo spaces, intended primarily to carry dry cargo in bulk.

### 4.1. General Specifications

The vessel selected as base case to present the fatigue assessment relating to CSR-BC by direct finite element analysis is a Handysize Double Side Skin (DSS) bulk carrier. The general principle specifications for the considered bulk carrier are shown in Table 4-1. The bulk carrier has notation A (BC-A) which means that vessel can carry dry bulk cargoes of cargo density  $1.0 \text{ t/m}^3$  and above with specified hold empty at maximum draught. The bulk carrier has six cargo holds. The number 1 of cargo hold is in the fore of the ship and No. 6 is in the aft of the ship. The hold No. 4 will be approximately located in the middle of the ship. The No. 4 cargo hold is designed for dual purposes of cargo hold & full water ballast tank. In addition, it can be empty at scantling draught. The midship section of the corresponding bulk carrier is shown in Figure 4-1.

Table 4-1: Bulk carrier principle specifications

Length over all (O.A)	190.00	m
Length (B.P.)	182.6	m
Scantling length	180.72	m
Breadth molded	23.6	m
Depth molded	14.6	m
Scantling draught (full load condition)	10.1	m
Draught (Normal ballast)	5.888	m
Draught (heavy ballast)	7.266	m
Block coefficient	0.855	-
Service speed	14.00	knots
Dead weight	30,000.00	tones
Frame spacing in cargo hold area	800	mm
Stiffener spacing	740	mm
Class notation	BC-A	-

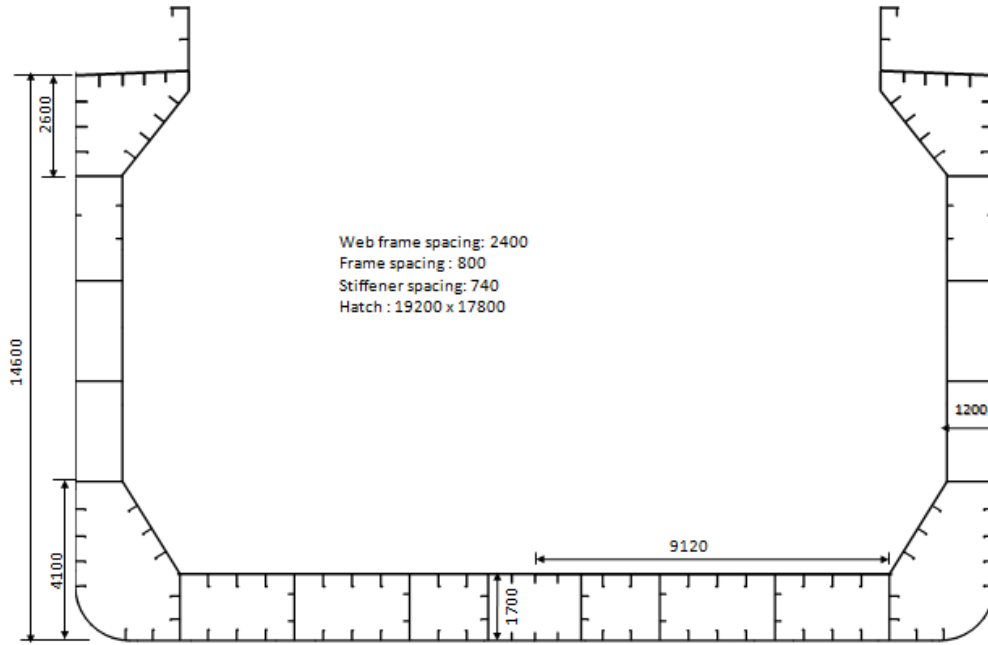


Figure 4-1 (a): Midship section of DSS bulk carrier

Note: The detail for thickness of plate and longitudinal stiffeners dimensions in Appendix A10

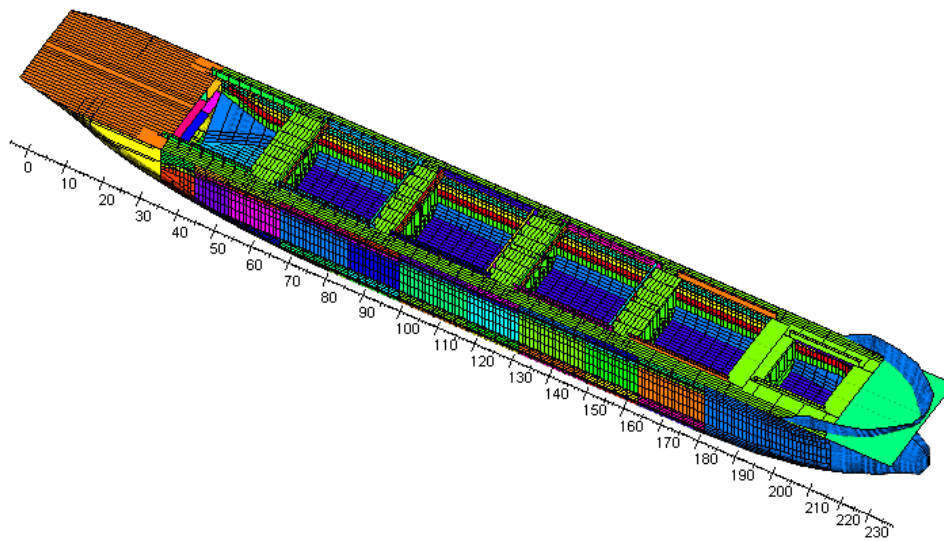


Figure 4-1(b): DSS bulk carrier

## 4.2 Critical Areas against Fatigue

Bulk carriers are faced many modes of cyclic forces that combine with other forces acting upon the vessel's structure. Over time these cyclic stresses, can weaken the vessel's structural capacity. Cyclic wave pressure act on upon the side frames of the vessel in a constant cycle of loading and unloading forces. For single bulk carriers carrying high density cargo, such as iron ore, the side frames do not have an internal pressure to counteract the external forces and the side shell forced inward by the unbalanced forces.

Similarly, the ordinary longitudinal stiffeners in upper and lower wing tanks and double bottom are subjected to fluctuating stresses due to the external wave action (static & dynamic) as well as the internal pressure from the ballast tanks. These longitudinals are also subjected to the fluctuating longitudinal hull girder stresses imposed by the passing wave along the length of the vessel. The toes of hatch coaming termination brackets are subjected to fluctuating hull girder vertical bending moment stresses and torsional wave induced stresses imposed by waves encountered at oblique wave heading. The actual fatigue crack in typical bulk carrier can be shown in Figure 4-2.

The areas of critical details prone to fatigue according to IACS rules are shown in Table 4-2.

Table 4-2: Members and locations subjected to fatigue strength assessment (CSR)

Members	Details
Inner bottom plating	Connection with sloping/or vertical plate lower stool
	Connection with sloping plate of hopper tank
Inner side plating	Connection with sloping plate of hopper tank
Transverse bulkhead	Connection with sloping plate of lower stool
	Connection with sloping plate of upper stool
Hold frames of single bulk carriers	Connection to the upper and lower wing tank
Ordinary stiffener in double side space	Connection of longitudinal stiffeners with web frames and transverse bulkhead
	Connection of transverse stiffener with stringer or similar
Ordinary stiffeners in upper and lower wing tank	Connection of longitudinal stiffeners with web frames and transverse bulkhead
Ordinary stiffeners in double bottom	Connection of longitudinal stiffeners with floors and floors in way of lower stool or transverse bulkhead
Hatch corners	Free edges of hatch corners

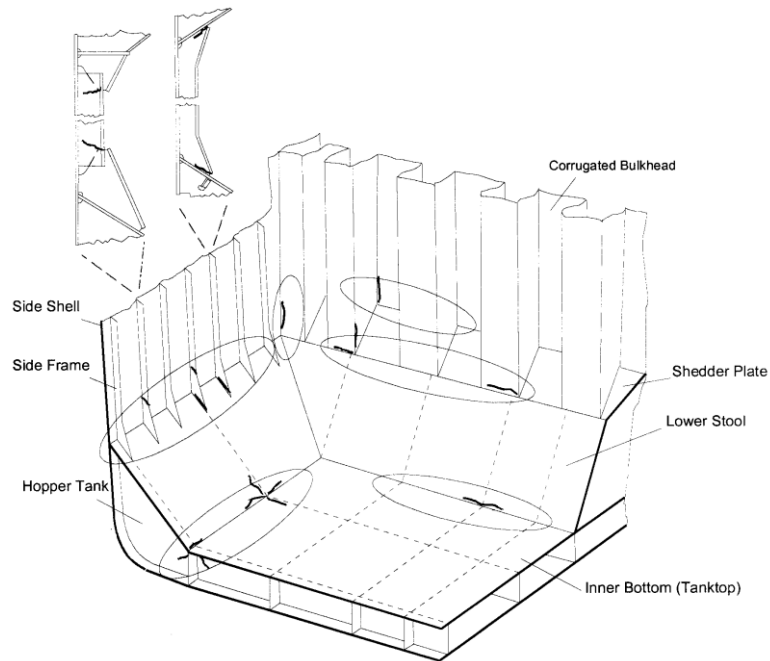


Figure 4-2: Fatigue crack locations and orientation in typical bulk carrier (SSC, 1999)

### 4.3. Load Calculation

When a vessel is sailing at sea with different loading conditions, it is subjected to various load patterns with many magnitudes which cause deformation of its structure, as well as fluctuating stresses. The aim of this section is to understand the type of design loads and its distribution that used in fatigue assessment according to CSR. In addition, to verify the Poseidon FEM model that created further. All design loads used in FEM fatigue analysis model according to CSR can be calculated automatically in Poseidon software modeling. The level of probability for design load to fatigue analysis respecting to IACS rules is  $10^{-4}$ .

The loads which have been affected on the structure of hull ship can be as follow:

- **Longitudinal loads-Global effect:** means the load concerning the overall strength of the ship's hull, such as the still water and wave bending moment, shear force and torsional moment acting on a hull girder and result in global displacements.

**-lateral loads-Local effect:** denote the loads which cause distortion of local members due to unbalance of external and internal loads, including structural and cargo weights and their dynamic effects. These loads can be categorized as following:

*External hydrostatic and hydrodynamic loads:* The hydrostatic load is static pressure from the water surrounding the hull of the vessel, which acts on the hull structure as an external load. Another external load is the hydrodynamic load induced by the interaction between waves and the ship motion. It is superimposed on the hydrostatic load and creates the total external water pressure.

*Structural weight, ballast water weight, fuel oil weight and cargo weight:* These loads are dead loads, which mean constant loads that are time independent, induced by gravity at the centers of gravity of the members.

*Inertia force of cargo or ballast due to ship motion:* The inertia force is induced by the reaction force of self weight, cargo weight or ballast weight due to the acceleration of the ship motion. Assume that a vessel is rolling among waves in a fully loaded condition. Then the cargo in each hold has a cyclic movement in the vertical and/or transverse direction. This must result in a fluctuating pressure of the hull structure of the hold due to the inertia force of the cargo movement. In addition, internal pressure is introduced not only by rolling but also by the ship's other motions, such as heaving, pitching, etc.

#### **4.3.1 Ship Motions and Accelerations**

Further down, in Table 4-3 all bulk carrier absolute motions and accelerations in full load, alternate load, normal ballast and heavy ballast conditions are calculated, using the equations given by IACS rules, i.e. (Roll, Pitch, Heave, Sway, Surge). In general, the values of ship motions and accelerations to be computed for fatigue are those which can be reached with a probability level of  $10^{-4}$ . The ship's relative accelerations will result according to the X, Y, and Z coordinates inserted. They will be computed for the longitudinal, transverse, and vertical directions for all loading conditions and all load cases, (H1, H2, F1, F2, R1, R2, P1, and P2) as shown in Figure 4-3. The roll radius of gyration and metacentric height for every load conditions are taken from the CSR rules but if these values are known from the designer. Then the design's values should be used.

Table 4-3: Bulk carrier motions and accelerations

	Full load	Alternate	Normal ballast	Heavy ballast
Roll period ( $T_R$ ) (s)	9.58	11.29	8.75	8.94
Single roll amplitude( $\Theta$ ) (deg)	14.68	14.06	14.98	14.91
Pitch period ( $T_P$ ) s	11.79	11.79	10.49	10.93
Single pitch amplitude ( $\Phi$ ) (deg)	5.34			
Acceleration parameter	0.205			
Heave ( $a_{heave}$ ) ( $m/s^2$ )	2.013			
Sway ( $a_{sway}$ ) ( $m/s^2$ )	0.604			
Surge ( $a_{surge}$ ) ( $m/s^2$ )	0.403			
Define point (X,Y,Z)	(86.9,0,8.5)			

Full Load Condition (Alternate)								
	H1	H2	F1	F2	R1	R2	P1	P2
	Head Sea		Follow Sea		Beam (port side)		Beam (port side)	
	Sagging	Hogging	Sagging	Hogging	(+)	(-)	(+)	(-)
$a_x$	0.626	-0.626	0.000	0.000	0.000	0.000	0.000	0.000
$a_y$	0.000	0.000	0.000	0.000	2.481	-2.481	1.348	-1.348
$a_z$	2.166	-2.166	0.000	0.000	0.676	-0.676	2.013	-2.013

Normal ballast								
	H1	H2	F1	F2	R1	R2	P1	P2
	Head Sea		Follow Sea		Beam (port side)		Beam (port side)	
	Sagging	Hogging	Sagging	Hogging	(+)	(-)	(+)	(-)
$a_x$	0.658	-0.658	0.000	0.000	0.000	0.000	0.000	0.000
$a_y$	0.000	0.000	0.000	0.000	2.804	-2.804	1.445	-1.445
$a_z$	1.914	-1.914	0.000	0.000	0.676	-0.676	2.013	-2.013

Heavy ballast								
	H1	H2	F1	F2	R1	R2	P1	P2
	Head Sea		Follow Sea		Beam (port side)		Beam (port side)	
	Sagging	Hogging	Sagging	Hogging	(+)	(-)	(+)	(-)
$a_x$	0.632	-0.632	0.000	0.000	0.000	0.000	0.000	0.000
$a_y$	0.000	0.000	0.000	0.000	2.692	-2.692	1.412	-1.412
$a_z$	1.983	-1.983	0.000	0.000	0.676	-0.676	2.013	-2.013

Figure 4-3: Ship accelerations



### 4.3.2 Hull Girder Load

The Hull girder load in Table 4-4 is in the mid-part of the ship ( $0.3 - 0.7 L$ ), these loads consist of still water bending moment, wave vertical and horizontal bending moment and wave vertical shear Force. In general, the value of still water bending moment and shear force are to be treated as the upper limits with respect to hull girder strength. In case the loading of the ship is known from the design the exact still water bending moment to be considered.

Table 4-4: Hull girder loads

Hull girder loads			
$C$	9.447	-	Wave Parameter
$L$	180.72	m	Length
$B$	23.6	m	Breadth
$C_B$	0.855	-	Block Coefficient
$P$	0.0001	-	Probability Level for fatigue
$f_p$	0.5	-	Probability Coefficient
$F_M$	1	-	
$T_{LC}$	10.1	m	Scantling draught (full load condition)
$M_{WV,H}$	591454	kN.m	Wave vertical bending moment (hogging)
$M_{WV,s}$	622765	kN.m	Wave vertical bending moment (sagging)
$M_{SW,H}$	1390071	kN.m	Still water vertical bending moment (hogging)
$M_{SW,s}$	1358760	kN.m	Still water vertical bending moment (sagging)
$M_{W,H}$	520046	kN.m	Wave horizontal bending moment
$Q_{WV}$	6579	kN	Wave vertical shear force

### 4.3.3 External Pressure

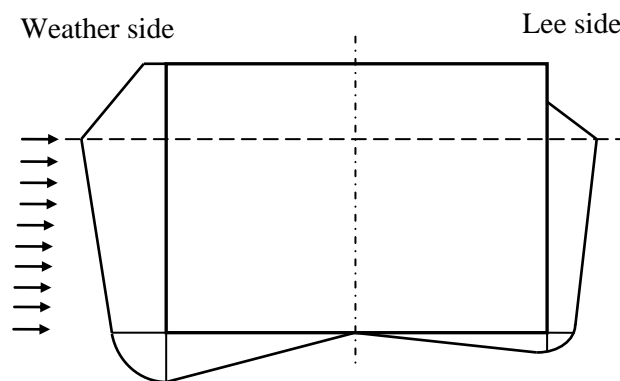
The external pressures have been calculated as seen in Table 4-5 according to the coordinates inserted  $x, y, z$  point (86.92, 11.8, 0) by user. Figure 4-4 shows the distribution of hydrodynamic external pressure at midship section when it is maximum.

The external pressure can divide in the following categories:

- Hydrostatic pressure
- Hydrodynamic pressure below water line
- Hydrodynamic pressure above water line
- External pressure on exposed deck

Table 4-5: Total external pressure at full loading condition

Full Load Condition		
Load case	Hydrodynamic pressure (kN/m <sup>2</sup> )	Total pressure (static & dynamic) (kN/m <sup>2</sup> )
H1	17.465	119.023
H2	-17.465	84.093
F1	-32.418	69.140
F2	32.418	133.976
R1	38.535	140.093
R2	-38.535	63.023
P1 (weather side)	60.776	162.334
P2 (weather side)	-60.776	40.782
Static pressure	101.558	

Figure 4-4: Distribution of hydrodynamic pressure  $p_1$  at midship

#### 4.3.4 Internal Pressure and loads

The internal pressures of a bulk carrier can be divided in still and lateral pressure induced by:

- Dry bulk cargo
- Water ballast

In order to obtain the pressure mentioned above some additional input data are needed to define the geometry of the area for both cases. The input necessary for the cargo hold are:

- Hold length ( $l_H$ )
- Hold breadth ( $B_H$ )
- Height of double bottom ( $h_{DB}$ )

- Vertical distance between inner bottom and lower interception of top side tank and side shell, ( $h_{HPU}$ ) as seen in Figure 4-5.
- Volume of hatch coaming ( $V_{HC}$ )
- Area above the lower interception of topside tank and side shell till the upper deck level, ( $S_o$ )
- Density of the cargo, ( $\sigma_c$ )
- X co-ordinate of the center of gravity of hold ( $x_G$ )
- Y co-ordinate of center of gravity of hold, ( $y_G$ )

Table 4-6 shown the inertia and static pressure due cargo in cargo hold number 4 at the top of inner bottom plate. All the previous calculations have been verified with GL Poseidon software for bulk carrier. It is found that there are no differences between the values from Excel sheet calculation and Poseidon for the same data.

Table 4-6: Inertia and still water pressure due cargo in hold No. 4

Inertia Pressure Due Cargo in Hold No.4 (Homogenous Full Load Condition)							
H1	H2	F1	F2	R1	R2	P1	P2
Head Sea		Follow Sea		Beam (port side)		Beam (port side)	
Sagging	Hogging	Sagging	Hogging	(+)	(-)	(+)	(-)
36.398	-36.398	0.000	0.000	11.369	-11.369	33.828	-33.828
Pressure in still water		164.879 kN/m <sup>2</sup>					

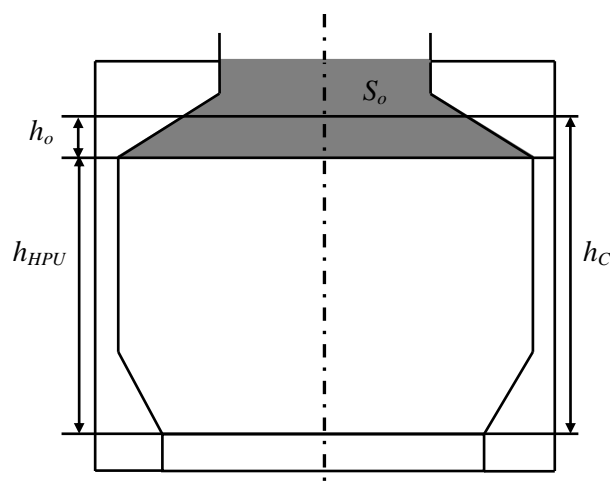


Figure 4-5: Double skin bulk carrier



## 5. GLOBAL FEM MODELING

The primary mission in developing the finite element model is to develop a model that can give best possible accurate predictions of fatigue strength in the critical details for the relevant bulk carrier under CSR-BC with feasible computation and working efforts. IACS CSR for Bulk Carriers contain guidelines on the procedure that and the type of elements which are used in order to develop a model for fatigue analysis. GL-POSEIDON and ANSYS software were used for fatigue assessment. The POSEIDON software is used to model structure of the bulk carrier, geometry, generate the fatigue loads complying with IACS Rules and coarse FEM model. The ANSYS code is used for fatigue analysis. This is a widely used commercial finite element code for structural and other analyses for general not ship-specific tool. This code was preferred because it is versatile, provides an extensive library of elements, several options for fatigue analysis post-processor and submodelling techniques.

On this thesis, two global models based on CSR-BC have been created for the three midship cargo holds. The first one is modeled using shell element for plate and beam element for stiffeners. The second one is modeled taking shell element for both plate and stiffeners. The purpose of global model is to obtain description about the distribution of stresses, to calculate global nominal stress and to interpolate the displacements into the boundaries of submodels. In addition, can used to refine the mesh in the critical detail areas for obtain the hot spot stress for fatigue assessment.

### 5.1. Model Description

In the following a brief description of the finite element model is provided. The geometry design, mesh generation and load application for fatigue assessment are all carried out using the POSEDION pre-processor for CSR bulk carrier. This program provides specific tools for geometric and finite element modeling for bulk carrier under IACS rules. GL-POSEIDON code is designed to support the calculation of scantlings for ship structures during the preliminary design and construction process. The scantlings criteria, i.e. the calculation of required dimensions and materials are performed in accordance to:

- Germanischer Lloyd Rules for Classification and Construction or IACS common structural rules for bulk carrier or tanker in the new version

- Direct Calculation Procedures (Finite Element Analysis)

The model consists of the following major parts:

- Double bottom
- Hopper and wing
- Outer shell and inner shell
- Deck and hatches
- Transverse bulk heads

The transverse bulk head consist of the following parts:

- Lower stool
- Upper stool
- Corrugations

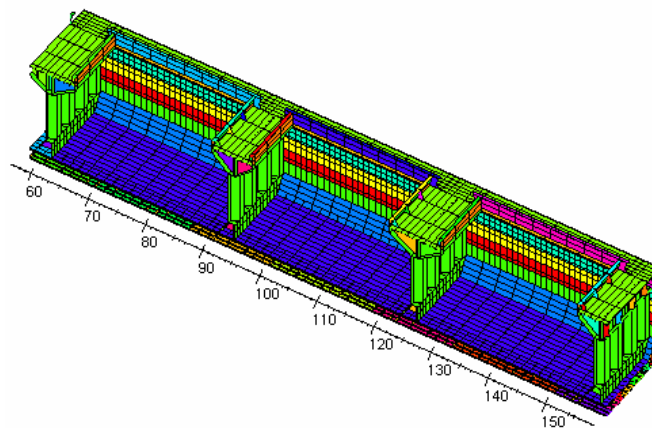


Figure 5-1: Half section in the geometry of global model

Figure 5-1 shows the half section of the longitudinal extent of FE model which to be cover three cargo holds and four transverse bulkheads. The transverse bulkheads at the ends of the model extent are to be included, together with their associated stools. Both ends of the model are to form vertical planes and to include any transverse web frames on the planes if any.

Fatigue strength assessment of a bulk carrier  
according to Common Structural Rules

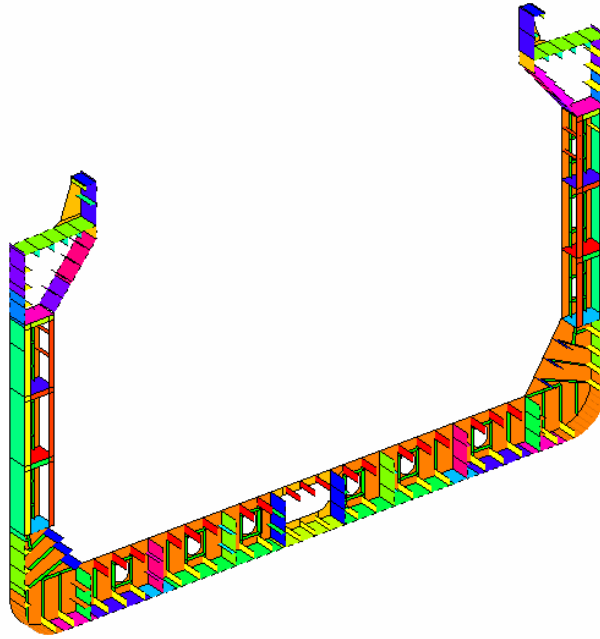


Figure 5-2: Midship web frame section

Figure 5-2 shows the midship web frame with supported stiffeners and how the longitudinal stiffeners are transferring the web frame floor. Also, the opening in traverse floor with supported stiffener.

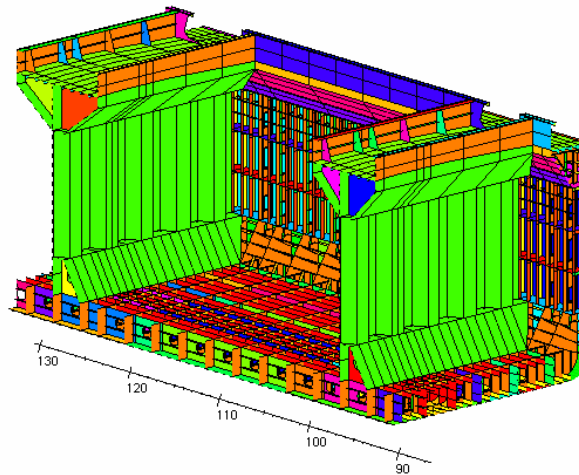


Figure 5-3: View of cargo hold No. 4 structural elements

Figure 5-3 shows the stiffening system in double bottom, the stringers and transverse stiffeners in the double side and the transverse bulk head elements. In addition, deck and hatch configuration. Large vertical brackets support the hatches.

## 5.2. Material Model

The material properties used in the analysis are based on nominal properties of steel used in the fabrication of bulk carrier. Three kind of steel are used in this vessel as following, mild steel, AH 32 and AH36 grade steel. The outer shell, inner shell and corrugated bulk head are constructed with high tensile strength steel grade AH32. The deck constructed with steel grade AH36. The materials considered properties are shown in Table 5-1.

Table 5-1: Material properties

Mat. No.	E-Modulus kN/m <sup>2</sup>	G-Modulus kN/m <sup>2</sup>	Density Kg/m <sup>3</sup>	Yield Stress N/mm <sup>2</sup>	Poisson's Ratio	Steel Grade
1	206000000	79230769	8000	235	0.3	MS
2	206000000	79230769	8000	315	0.3	AH32
3	206000000	79230769	8000	355	0.3	AH36

## 5.3. Boundary Conditions

Both ends of the model are to be simply supported according to CSR. The nodes on the longitudinal members at both end sections are to be rigidly linked to independent points at the neutral axis on the centerline as shown in Table 5-2. The independent points of both ends are to be fixed as shown in Table 5-3.

Table 5-2: Rigid-link of both ends (CSR-BC)

Nodes on longitudinal members at both ends of the model	Translational			Rotational		
	Dx	Dy	Dz	Rx	Ry	Rz
All longitudinal members	RL	RL	RL	-	-	-
RL means rigidly linked to the relevant degrees of freedom of the independent point						

Table 5-3: Support condition of the independent point (CSR-BC)

Location of the independent point	Translational			Rotational		
	Dx	Dy	Dz	Rx	Ry	Rz
Independent point on aft end of model	-	Fix	Fix	Fix	-	-
Independent point on fore of model	Fix	Fix	Fix	Fix	-	-



The boundary conditions that implemented in the Poseidon global model are according to CSR for Bulk Carriers. The nodes at both end cross sections are to be rigidly linked by constraint equations (CE) to an independent point at neutral axis on centerline. The independent points at both ends are to be fixed according Table 5-3. The coarse model for the three hold cargo is extended from frame number 57 to frame number 158. In addition, the frame spacing is 800 mm. The user must select at the end cross sections the “y-z-plane with CE”. For the support condition the unit force (code 2) must be select for the columns y, z, yy and zz. With this command also the independent point will be created and supported in the necessary directions as shown in Table 5-4.

Table 5-4: End section boundary condition

Model No		Item		Location of Section			Support Condition						Boundary Value
Kind of Section		X-Start	X-End	Y-Z Start	Y-Z End	Sym	X	Y	Z	XX	YY	ZZ	
y-z-plane with CE		57					0	2	2	0	2	2	1.00000e+008
y-z-plane with CE		158					0	2	2	0	2	2	1.00000e+008
* y-z-plane with CE		158					0	2	2	0	2	2	1.00000e+008

## 5.4. Load Analysis

There are four standard loading conditions for fatigue assessment for bulk carrier type A (BC-A) under common structural rules.

- Full load condition
- Alternate heavy load condition
- Normal ballast condition
- Heavy ballast condition

In addition, for every load condition there are eight load cases as shown in Table 5-5.

Table 5-5: Definition of load cases (CSR-BC)

Load case	H1	H2	F1	F2	R1	R2	P1	P2
EDW	“H”		“F”		“R”		“P”	
Heading	Head		Follow		Beam (port: weather side)		Beam (port: weather side)	
Effect	Max. Bending Moment		Max. Bending Moment		Max. Roll		Max. Ext. Pressure	
	Sagging	Hogging	Sagging	Hogging	(+)	(-)	(+)	(-)

Regarding local loads, external (hydrostatic and hydrodynamic) pressures and internal (static and inertial) pressures are considered as lateral loads in still-water and in waves. The internal static pressures are induced by the weights carried, while the internal inertial pressures are induced by the accelerations on the masses and calculated with relevant load combination factor (LCF).

## 5.5. Poseidon Model

In POSEIDON software the fuel oil, ballast tanks and cargo holds are modeled by compartments. The compartment represents the geometry/topology of tank or hold and composed out of cells at different cross sections as shown in Figure 5-4.

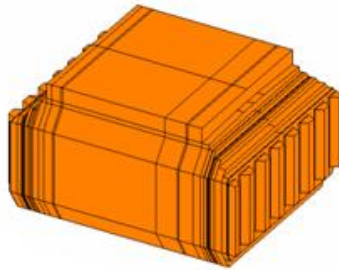


Figure 5-4: Cargo hold No. 4 compartment model

After the creation of compartments which represent general arrangement in the modeled area as shown in Figure 5-5. The volume and position of centre of gravity for each tank/hold is checked automatically and compared with the actual data in Table 5-6. There is slightly difference between them.

Table 5-6: Cargo holds/tanks volume

Hold /Tank	Volume m <sup>3</sup>	L.C.G m	T.C.G m	V.C.G m
No.3 Cargo Hold	7106.8	112.33	0.0	8.66
No.4 Cargo Hold	7105.2	86.6	0.0	8.66
No.5 Cargo Hold	710.68	61.3	0.0	8.66
No.3 WBTKP	961.1	112.8	8.8	4.86
No.3 WBTKS	961.1	112.8	-8.8	4.86
No.4 WBTKP	616.4	87.20	10.84	7.11
No.4 WBTKS	616.4	87.20	-10.84	7.11
No.5 WBTKP	509.9	61.60	-10.94	8.4
No.5 WBTKS	509.9	61.60	-10.94	8.4
No.1 HFOTKP	344.7	87.2	5.16	0.85
No.1 HFOTKS	344.7	87.2	-5.16	0.85
No.2 HFOTKP	413.4	60.21	6.29	0.87
No.2 HFOTKS	413.4	60.21	-6.29	0.87

Fatigue strength assessment of a bulk carrier  
according to Common Structural Rules

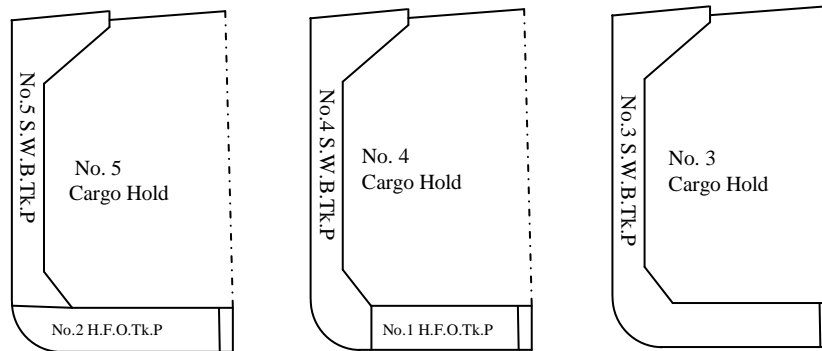


Figure 5-5: General arrangement of midship

Content of compartments wizard has been used afterwards to define the content of each compartment. In this procedure each tank was referred to its compartment and specified, if it is ballast or fuel tank, by selecting its type from the medium choices. Once the type has been defined the other parameters such as Rho, length, width, location of the tank, and height of over flow has been done manually as presented in Figure 5-6.

Frame No.		F/A		A+F						
Tank No.	Comp. Name	Rho [t/m <sup>3</sup> ]	pv [bar]	Length [m]	Frame No. Aft	Yp [m]	Ys [m]	Height of overflow [m]		Full Name
Sym.	Medium	Ballast Exc		Width [m]	Forward	Zp [m]	Zs [m]			
P	1 Comp:SWBT3P	1.025	0.000	25.60	125	11.800	8.900	15.360		
	Ballast	Sequential		10.600	157	14.600	14.718			
S	2 Comp:SWBT3S	1.025	0.000	25.60	125	-8.900	-11.800	15.360		
	Ballast	Sequential		10.600	157	14.718	14.600			
P	3 Comp:SWBT4P	1.025	0.000	25.60	93	11.800	8.900	15.360		
	Ballast	Sequential		2.900	125	14.600	14.718			
S	4 Comp:SWBT4S	1.025	0.000	25.60	93	-8.900	-11.800	15.360		
	Ballast	Sequential		2.900	125	14.718	14.600			
P	5 Comp:SWBT5P	1.025	0.000	25.60	61	11.800	8.900	15.360		
	Ballast	Sequential		2.900	93	14.600	14.718			
S	6 Comp:SWBT5S	1.025	0.000	25.60	61	-8.900	-11.800	15.360		
	Ballast	Sequential		2.900	93	14.718	14.600			
P	7 Comp:HFOT1P	0.880	0.000	25.60	61	11.800	1.200	15.360		
	Fuel Oil			10.600	93	1.700	1.700			
S	8 Comp:HFOT1S	0.880	0.000	25.60	61	-1.200	-11.800	15.360		
	Fuel Oil			10.600	93	1.700	1.700			
P	9 Comp:HFOT2P	0.880	0.000	25.60	93	9.120	1.200	15.360		
	Fuel Oil			7.920	125	1.700	1.700			
S	10 Comp:HFOT2S	0.880	0.000	25.60	93	-1.200	-9.120	15.360		
	Fuel Oil			7.920	125	1.700	1.700			
	11 Comp:CH_4	1.025	0.000	25.60	93	8.900	-8.900	15.360		
	Ballast Cargo	Sequential		21.200	125	16.400	16.400			
*	11 Comp:CH_4	1.025	0.000	0.00	93	8.900	-8.900	15.360		
	Ballast Cargo	Sequential		21.200	125	16.400	16.400			

Figure 5-6: Configuration of ballast/fuel tanks content

The maximum design cargo loading for the considered bulk carrier is shown in Table 5-7.

Table 5-7: Maximum loading in cargo hold

Cargo Hold No.	3	4	5
Load(t/m <sup>2</sup> )	21.5	20.0	24.5
Max. Cargo Mass (t)	10300	7950	11605

According to CSR-BCA for Fatigue-MH case, the cargo density for calculation of dry cargo pressure is defined by the actual cargo mass in a cargo hold corresponding to homogeneously loaded condition at maximum draught, in tones divided by Volume, in m<sup>3</sup>, of cargo hold excluding the volume enclosed by hatch coaming. Also, for Fatigue-Alternate case, the cargo density 3.0 t/ m<sup>3</sup> is to be used for calculation of dray cargo pressure as shown in Figure 5-7.

No.	Item	Plane Load			Wheel Load		CargoType		
		Frame No. Aft	Upper Edge [m]	Static Load [kN/m <sup>2</sup> ]	Sea. Load [kN]	Sea. Area [m <sup>2</sup> ]	Mass [t]	hc [m]	
Holdno.	Comp. Name	Deck No.	Forward	Repose Angle [deg]	Density C. <sub>1</sub> [t/m <sup>3</sup> ]	Harb. Load [kN]	Harb. Area [m <sup>2</sup> ]	Mass [t]	hc [m]
1	Fatigue		61		0.0			Fatigue-MH	
5	Comp:CH_5	1	93	30	1.638898			11605	14.900
2	Fatigue-Alt		61		0.0			Fatigue-Alternate	
5	Comp:CH_5	1	93	30	3.00			11605	7.766
3	Fatigue		93		0.0			Fatigue-MH	
4	Comp:CH_4	1	125	30	1.128111			7950	14.900
4	Fatigue		125		0.0			Fatigue-MH	
3	Comp:CH_3	1	157	30	1.461379			10300	14.900
5	Fatigue Alt		125		0.0			Fatigue-Alternate	
3	Comp:CH_3	1	157	30	3.00			10300	6.964
6	M-Full		125		0.0			M-Full	
3	Comp:CH_3	1	157	30	1.46				14.900
7	M-Full		61		0.0			M-Full	
5	Comp:CH_5	1	93	30	1.64				14.900
8	M-Full		93		0.0			M-Full	
4	Comp:CH_4	1	125	30	1.13				14.900
9	M-Full		93		0.0			M-Full	
*	4	Comp:CH_4	1	125	30	1.13			14.900

Figure 5-7: Configuration of cargo hold loading for fatigue assessment

After that the POSEIDON software will be automatically calculate all global load cases for fatigue assessment according to CSR-BC with the possibility to adjust the metacentric height and roll radius of gyration for the considered loading condition.

### 5.5.1 Mesh Generation

The principle for selection of element type relating to CSR-BC is given below:

- (1) Stiffeners are to be modeled by beam or bar element having axial, torsional, bi-directional shear and bending stiffness. However, web stiffeners and face plates of primary supporting members may be modeled by rod element having only axial stiffness and a constant cross-sectional area along its length.
- (2) Plates are to be modeled by shell element having out-of-plane bending stiffness in addition to bi-axial and in-plane stiffness. However, membrane element having only bi-axial and in-plane stiffness can be used for plates that are not subject to lateral pressures.

For membrane and shell elements, only linear quad or triangle element are will be used, as shown in Figure 5-8. Triangle elements are to be avoided as far as possible, especially in highly stressed areas and in such areas around openings, at bracket connections and at hopper connections where significant stress gradient should be predicted.

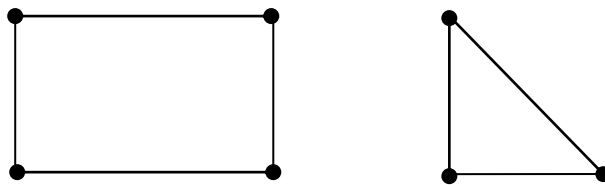


Figure 5-8: Shell quad and triangle elements

There are two modes in POSEIDON can be used to model the element as following:

- **Mode 3:** Plates are modeled as shell elements. Nodes are generated for the trace curves of the stiffeners and the stiffeners are modeled as beam elements.
- **Mode 4:** Plates are modeled as shell elements. Stiffeners webs are modeled in the same way as plates. The flange is modeled as truss element.

Most classification societies indicate the maximum distortion values for the elements, which can be used for evaluation of the model that has been designed. However, IACS does not refer to a way of evaluation of the F.E model rather than the aspect ratio of the elements that is not to exceed 1:4.

ABS, (American Bureau of Shipping), guidelines for the verification of the model was followed, these are:

- Aspect ratio should be less than 3
- Taper should be less than 10
- Internal angles should not be less than 30 degrees
- No free edge caused by wrong element connectivity
- Coincident nodes should be merged
- No coincident elements should exist

The first model as shown in Figure 5-9 was created according to the specifications of the IACS rules for bulk carrier and is consisted of 85,437 elements. The number of shell elements is 59,467 and the number of beam elements is 25,970. The outer shell, inner shell and primary supporting members were modeled using plate element. However, beam element was used for all the stiffeners. The size of shell element is 800 x 740 mm and for hopper plate is 800 x 600 mm. The spacing of longitudinal stiffener is 740 mm, and only one element lies between two longitudinal stiffeners. The frame spacing is 800 mm. IACS indicates that the mesh size is to be equal to or less than the representative longitudinal stiffener or transverse side frame spacing.

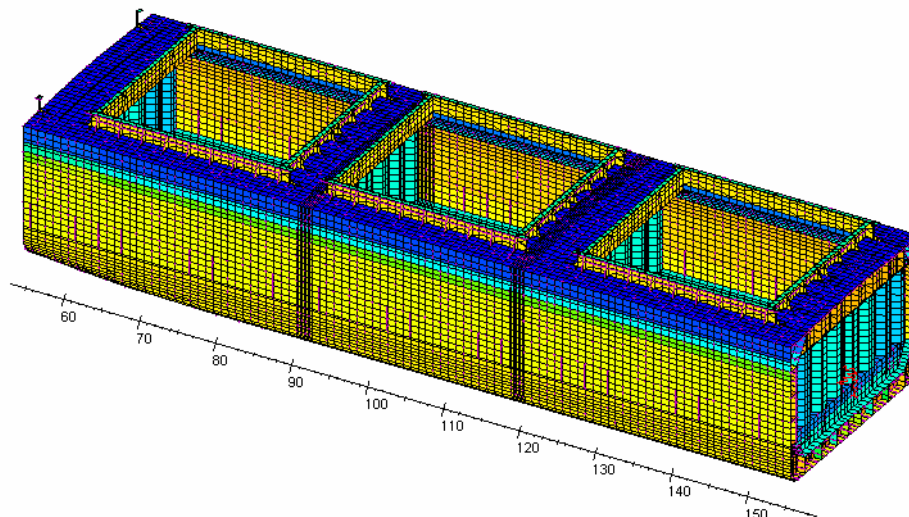


Figure 5-9: First model with shell element for plate and beam element for stiffener

The second model as shown in Figure 5-10 created like first according to CSR-BC rules but the outer shell, inner shell, primary supporting members and web stiffeners were modeled by shell element. The model contains 99,935 elements. The size of shell element is 800 x 740 mm.

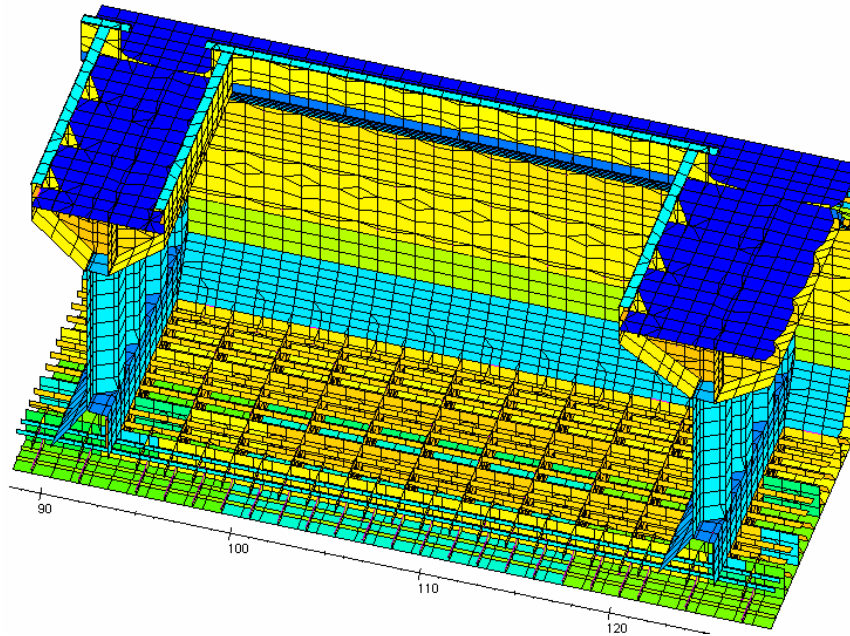


Figure 5-10: Second model-view of inner bottom stiffener mesh

There were some difficulties in meshing to use less coarse mesh and avoid the triangle element in some positions especially in the second model when used shell element for plate and stiffener due to limitation of number of element used in POSEIDON software and complex geometry like hopper web plate and opening. However, in the two models none of elements exceeded the maximum distortion values given from the classification societies and the mesh size within the limit of frame spacing or stiffener spacing even less in some places.

After the generation of the FE-model, there are two steps are necessary for load application in POSEIDON software. In the first step, all unit groups (e.g. static sea pressure, dynamic cargo pressure ...) are generated and reaction forces and moments are derived for each unit group. In a second step the bending moment distribution, based on local loads, is derived and additional moments at the end cross section of the 3-hold model are calculated in order to adjust the bending moment of the centre hold to the target value. After that, the nodal forces of each loading condition for fatigue assessment according to CSR-BC, CH4, and App.3 Tables are written to the FE-model

## 5.6. ANSYS Model

The Poseidon software model will be exported to the ANSYS. The constrain equation which present the boundary condition at both end cross sections not presented and the implementing of boundary conditions in ANSYS as following. Planar boundary condition will be applied to the ends of three cargo hold model. This is achieved through multi-point constraint (MPC) with master point located at the neutral axis height and slave points at the ends of the continuous longitudinal structures. MPC can be used to link the master and slave points at degree of freedom 2, 5, 6 or 1, 2, 3 as shown in Figure 5-11. The master points are fixed according to CSR and the slave points are rigidly linked to the master point at both end cross section.

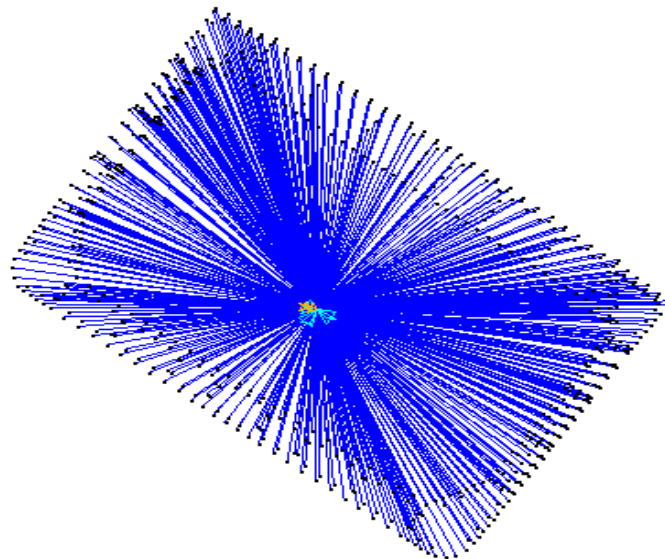


Figure 5-11: Boundary at end plane

The type of shell element which presented in the ANSYS and POSEIDON models called SHELL63. SHELL63 has both bending and membrane capabilities. Both in-plane and normal load are permitted. The element has six degree of freedom at each node, three translations and three rotations about X, Y, Z axis.



Fatigue strength assessment of a bulk carrier  
according to Common Structural Rules

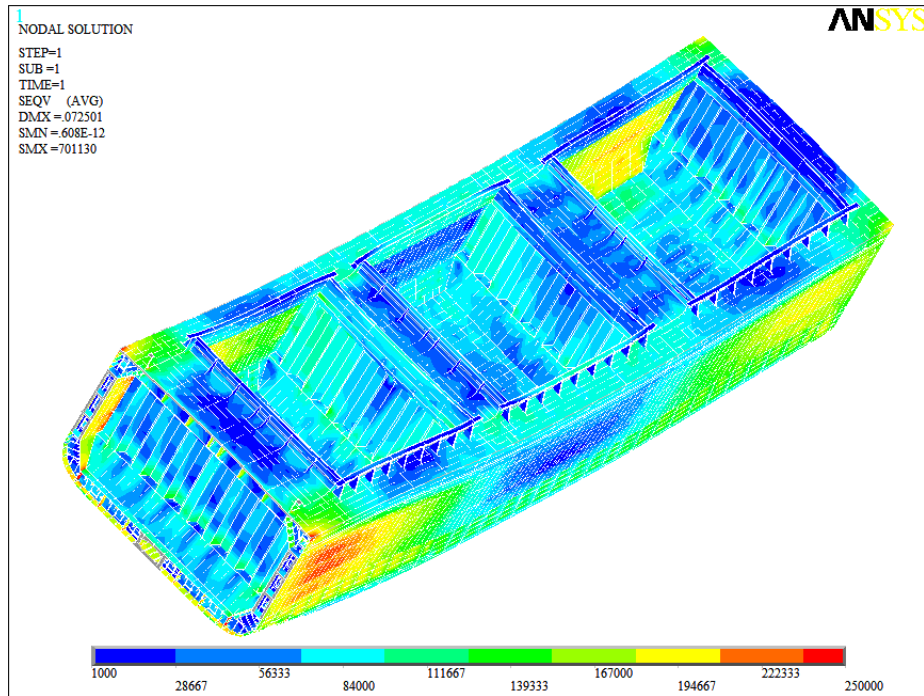


Figure 5-12: Von Misses stress in full load condition (sagging heading sea case)

Figure 5-12 shows the von misses stress distribution in the three hold model with mid-hold as the target for fatigue assessment. The unit of stress represented in this figure is in  $\text{kN/m}^2$ . The figure has shown the von misses' stress at center of shell element is less than the minimum yielding stress  $235 \text{ N/mm}^2$ .



## 6. SUBMODELLING

Submodelling is a technique most useful when it is necessary to obtain an accurate and detailed solution in a local region of a large model. In this method, global analysis using a relatively coarse mesh is first run, and then the local region of interest is created as submodel and analyzed separately with fine meshes taking into account of the effect of the rest part of the structure. By the way to consider the effect of the rest part of the structure upon the sub-region, submodelling procedures can be classified into several categories. Among those, specified boundary condition methods are most popular, in which state variables are transferred from global solution to determine the boundary response of the submodel for representing the effect of the rest part of the structure. Two methods can be classified into this category. Applying stress boundary condition method involves applying traction forces derived from stresses obtained by global analysis to the submodel boundary. Alternatively, in applying displacement boundary condition method, displacements are interpolated from the global solution at the boundary nodes of submodel grid (Mitsuru; et al., 2002).

It is also possible to model the coarse model with shell elements and the sub model with solid elements, which will keep the number of elements low and save time for solving the model. In the flowing sections the two decided critical details for submodelling hopper inner bottom knuckle and longitudinal stiffener web frame connection will be created and analyzed for fatigue assessment. Moreover, the applying displacement boundary condition method will be used for that analysis. The procedure for using the submodelling is as follow:

- Create and analyze the coarse model.
- Create the submodel.
- Perform the cut boundary interpolation
- Analyze the subomdel.
- Verify the distance between the cut boundaries and stress concentration is adequate

## 6.1. Hopper Inner Bottom Knuckle Submodel

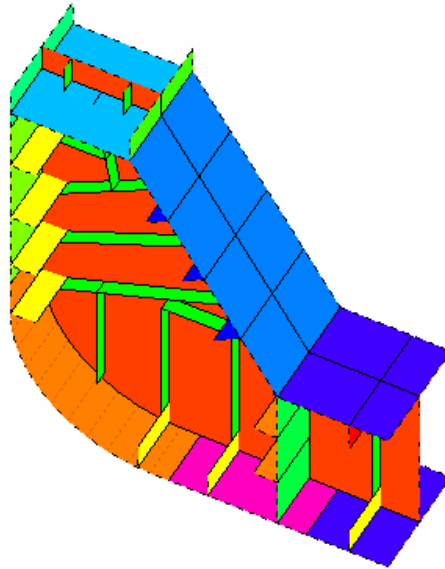


Figure 6-1: Hopper inner bottom knuckle geometry

The model of hopper inner bottom knuckle extend in x direction from frame 110 +200 (88.2 m) to frame 112 -200 (89.4 m), in y direction from 8.01 m to 11.8 m portside and in z direction from 0 to 4.4 m. Moreover, the model firstly generated from the global model in the POSEIDON software as shown in Figure 6-1 and exported as geometry to ANSYS. The local submodel is meshed with refined mesh. The mesh size is  $t \times t$  where  $t$  the thickness in mm of inner bottom plate as shown in Figure 6-2.

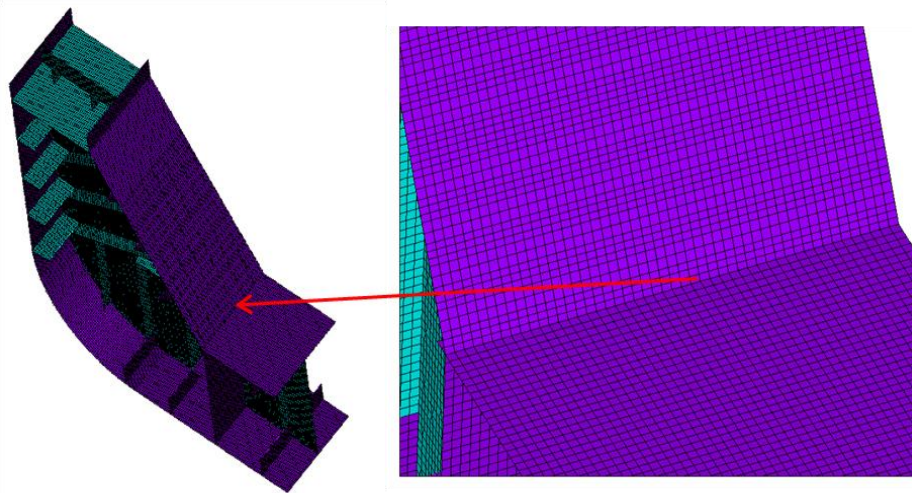


Figure 6-2: Hopper inner bottom knuckle mesh

3

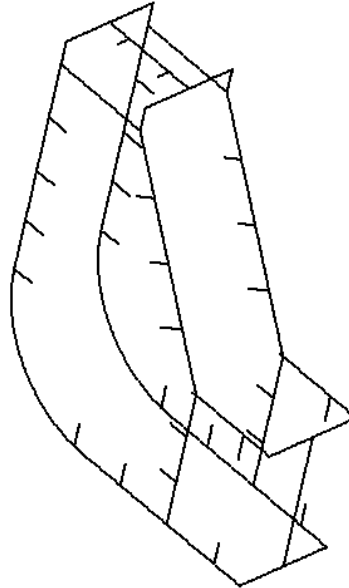


Figure 6-3: Hopper inner bottom model cut boundaries

Figure 6-3 shows the cut boundaries nodes of the submodel after meshing. The nodes are very dense. Afterward, the displacement from the global solution is interpolated into the cut boundaries of submodel as shown in Figure 6-4.

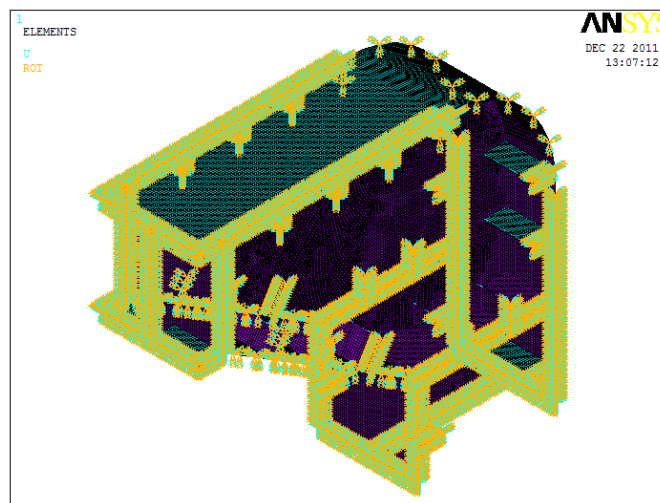


Figure 6-4: Displacement interpolation from global model to local model

The hopper inner bottom connection model is analyzed after interpolated the displacement. The Figure 6-4 shows the distribution of first principal stress (surface stress) in the coarse model and the fine model. The stress range distribution in the coarse model is between  $-10\text{N/mm}^2$  to  $200\text{N/mm}^2$ . The distribution of stress in fine model starts from  $200\text{N/mm}^2$  to  $500\text{N/mm}^2$ . This indicates that the stress distribution excluding the knuckle which represents the hot spot is satisfying with the coarse model.

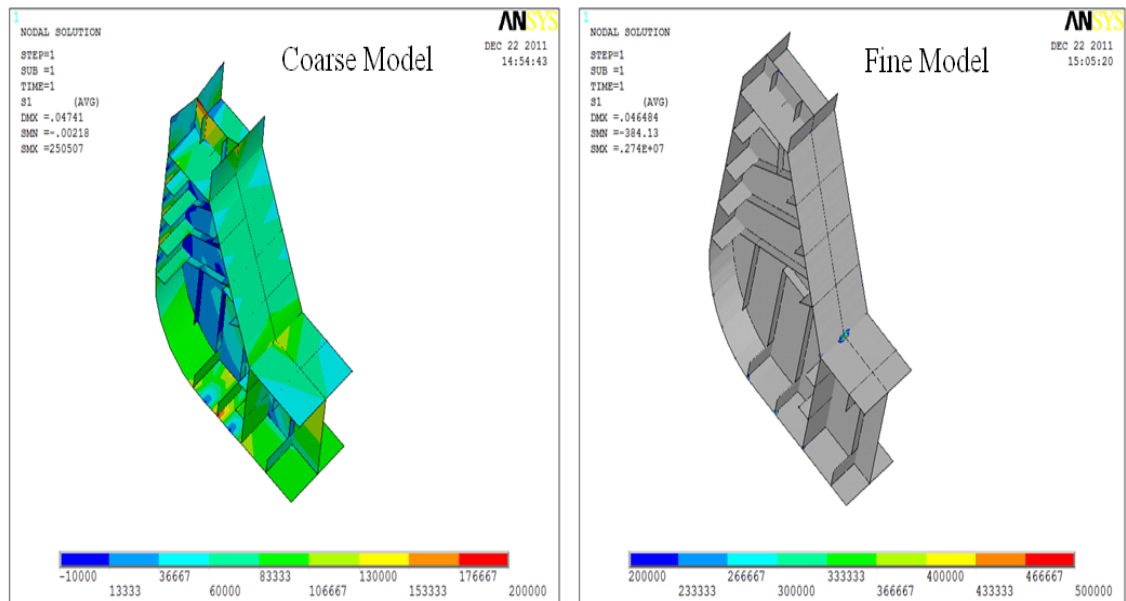


Figure 6-5: First principal stress in fine and coarse model

## 6.2. Longitudinal Stiffener Web Frame Connection Submodel

The following critical detail is presented the bottom longitudinal stiffener connection to transverse web frame and bulk head. The model extend in x direction from frame 93 -1200 (73.2 m) to frame 93 +1200 (75.6 m) (web frame spacing = 2400 mm), in y direction from 5.04 m to 5.78 m (stiffener spacing =740 mm), in z direction from 0 to 1 m. The Holland bulb profile (HP 260 mm x 11 mm) of the longitudinal stiffener is modeled by using equivalent angle profile. The section of the equivalent angle is obtained by using CSR Rules in Chapter 3 Section 6-4.1. Furthermore, the cutout and the collar plate connection are created as seen in Figure 6-6. The model has been created in ANSYS with the same global reference coordinate system in the coarse model. The model is meshed with fine mesh  $t \times t$  where  $t$  is the thickness of bottom plate shell as shown in Figure 6-7.

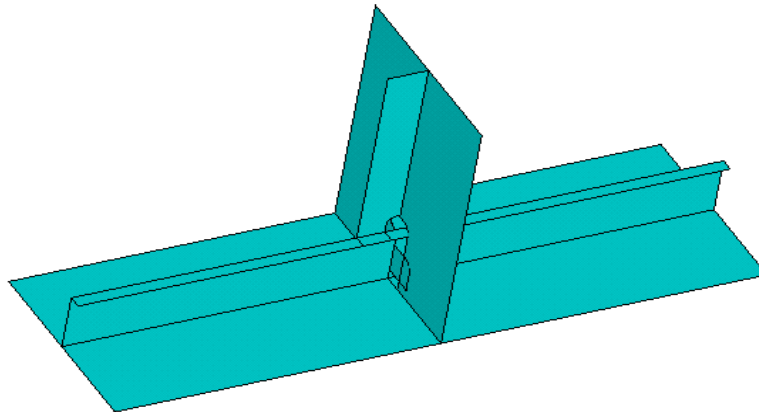


Figure 6-6: Longitudinal-web frame connection model

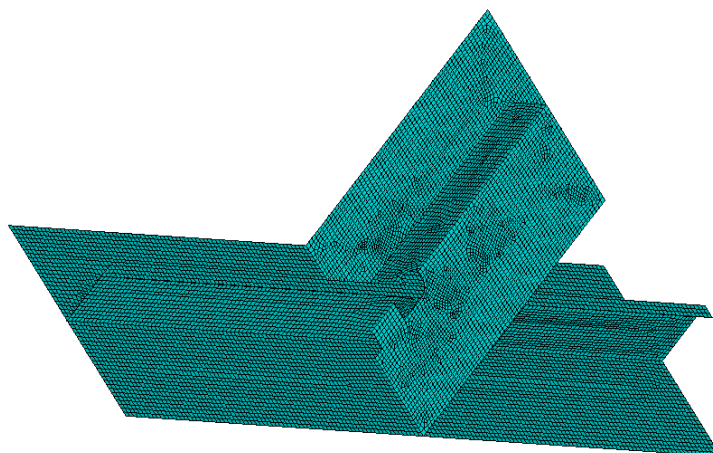


Figure 6-7: Longitudinal-web frame local model mesh

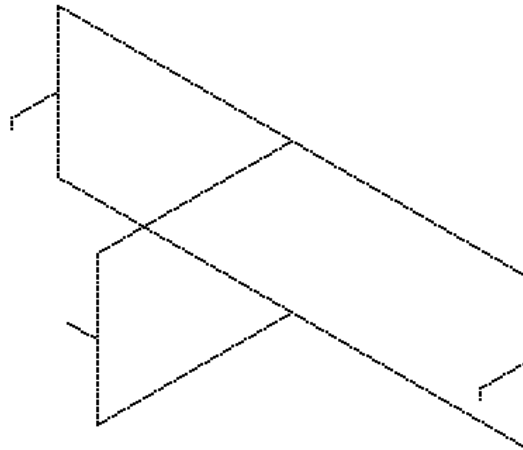


Figure 6-8: Longitudinal stiffener web frame model cut boundaries

Figure 6-8 and Figure 6-9 show the cut boundaries nodes in the longitudinal-web frame submodel and the distribution of third principal stress. It has been shown that the hot spot in compression and the longitudinal stiffener with attached plate is bending

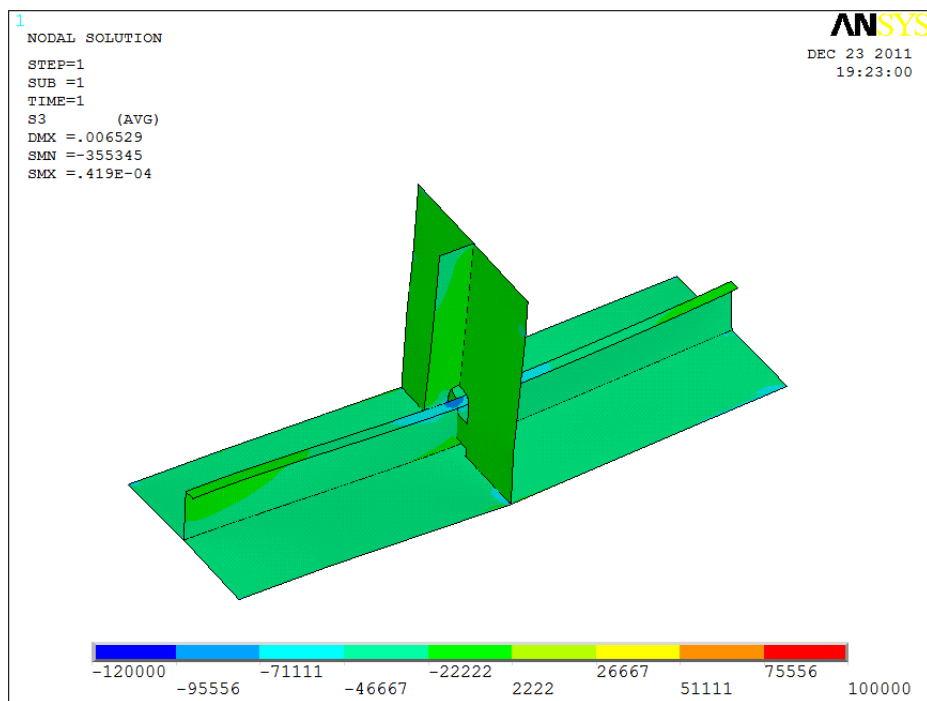


Figure 6-9: Third principal stress distribution in longitudinal-web frame local model



## 7. RESULTS AND ANALYSIS

The following sections will describe in more detail the procedure how the hot spot stress is extrapolated for the two previous submodels created in Chapter 6, hopper inner bottom knuckle and longitudinal stiffener web frame connection. The hot spot will be estimated for the two critical details considered and the geometry stress concentration factor will be evaluated by the direct FEM analysis and compared with the values at IACS rules. In addition, the cumulative fatigue damage for hopper-web frame knuckle is calculated considering all loading conditions with respecting load cases.

### 7.1. Hot Spot Stress Extrapolation

Hot spot stresses are determined using extrapolation procedure according to DNV Classification Notes No. 30.7 (DNV, 2010a). The following is a summary of these notes:

- Linear extrapolation of the stresses to the hot spot position from the points at  $t/2$  and  $3t/2$  will be illustrated, where  $t$  is the thickness of plate at weld toe or the hot spot stress is taken as the stress at point  $t/2$  multiplied by 1.12.
- The maximum absolute principal stress value within  $\pm 45^\circ$  of the normal of the weld will be used for evaluation of hot spot stress. Note that, principal stress is the normal stress to a plane, on which the stress becomes maximum or minimum.
- In model with 4-node shell element and  $t/2 \leq \text{element size} \leq t$ . Element surface stress at midpoint element is used. The stress at center point of element is extrapolated to line A-A to read out the stress at these points as shown in Figure 7-1.

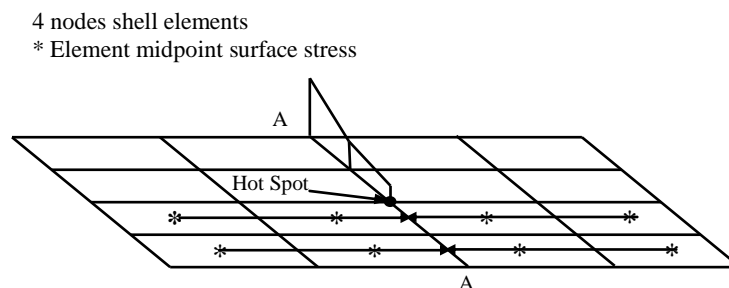


Figure 7-1: Hot spot stress extrapolation

Figure 7-2 shows the hot spot in hopper inner bottom knuckle model. Different load cases are investigated to decide which surface will be used, top or bottom surface of element. After that investigation the bottom element surface has the larger principal stress.

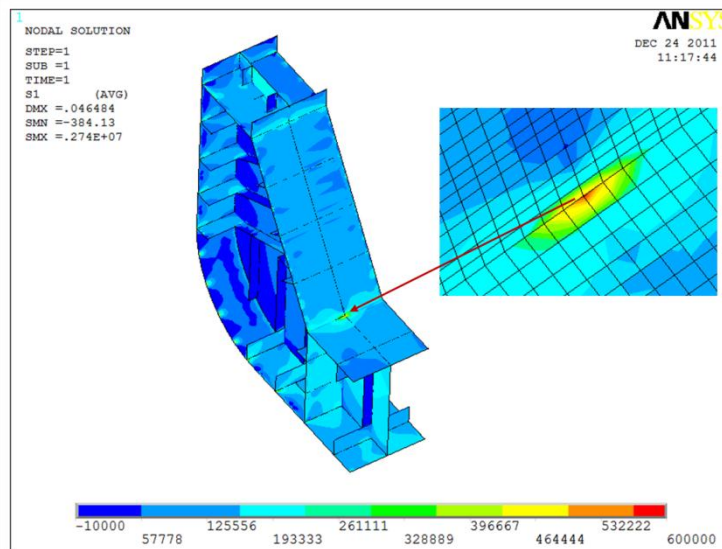


Figure 7-2: Hot spot at hopper Inner bottom knuckle

The direction of the principal stress is observed as seen in Figure 7-3 to found the maximum absolute principal stress among the three principal stresses (S1, S2, and S3) with direction within  $\pm 45^\circ$  from the normal of weld. For that case, the first principal stress has the largest value. In ANSYS code S1 is the most positive (tensile), S3 is the most negative (compressive) and S2 is in between the two other principal stresses major S1 and minor S3. Then it is always looking for S1 and S3 to found the maximum absolute value.

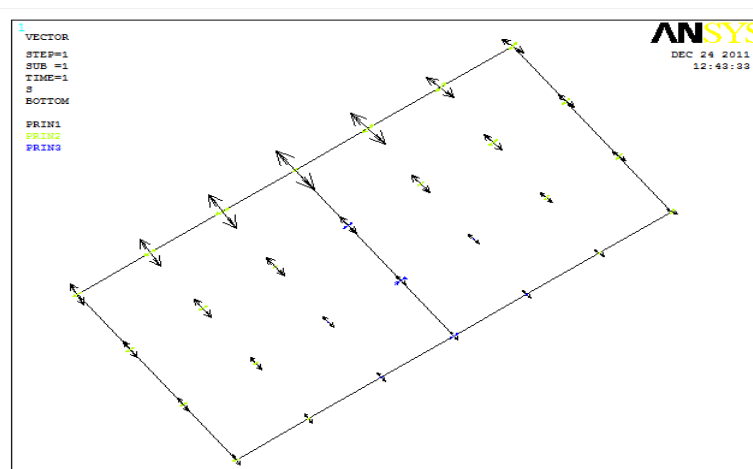


Figure 7-3: Vectors of principal stresses at element nodes

## 7.2. Geometry Stress Concentration Factor

Due to local geometry, stress concentration will occur at the considered details. This together with a complex load pattern makes it necessary to perform FEM analysis for these details to obtain information about the local stress concentrations. The modeling will contain the geometry of the local detail itself neglecting the weld geometry. The resulting  $K$ -factor,  $K_g$  will then represent the stress concentration caused by local geometry of the structure.

Hence, for design analysis a simplified numerical procedure is used in order to reduce the demand for fine mesh model for the calculation of  $K$ -factors. The  $K$ -factor can be calculated in two steps:

1. By fine mesh model using shell element as in that paper (or alternatively solid element). The stress concentration due to geometry effect of actual detail is calculated resulting in  $K_g$  factor.
2. The stress concentration due to the weld itself,  $K_w$  factor, is evaluated based on standard values available in all classifications notes or direct finite element calculations with very fine mesh of solid elements (weld radius has to be modeled).

The aim of the finite element analysis in this thesis is not to calculate the notch stress at a detail but to calculate the geometric stress distribution in the region of hot spot such that these stress can be used either directly in the fatigue assessment of a considered details or as a basis for derivation of geometry stress concentration factors. The stress concentration factor due to geometry effect is defined as,  $K_g = \sigma_g / \sigma_{nominal}$ . Where  $\sigma_g$  is the hot spot stress due geometry effect and  $\sigma_{nominal}$  is the nominal stress in the structure.

### 7.2.1 $K_g$ -Factor for Hopper Inner Bottom Knuckle

The element center point stress values of first principal stress from the hot spot presented in Figure 7-4. The value of hot spot evaluated according to the previous described DNV notes. The value at hot spot position is founded equal to  $644\text{N/mm}^2$ .

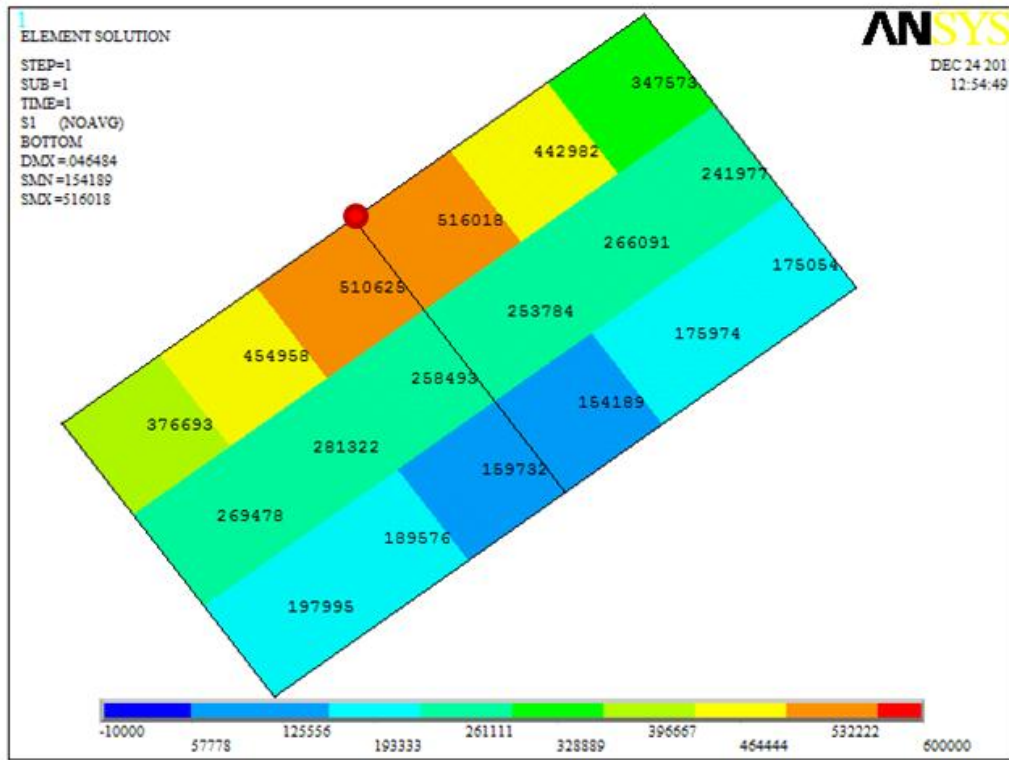


Figure 7-4: First principal element midpoint stress

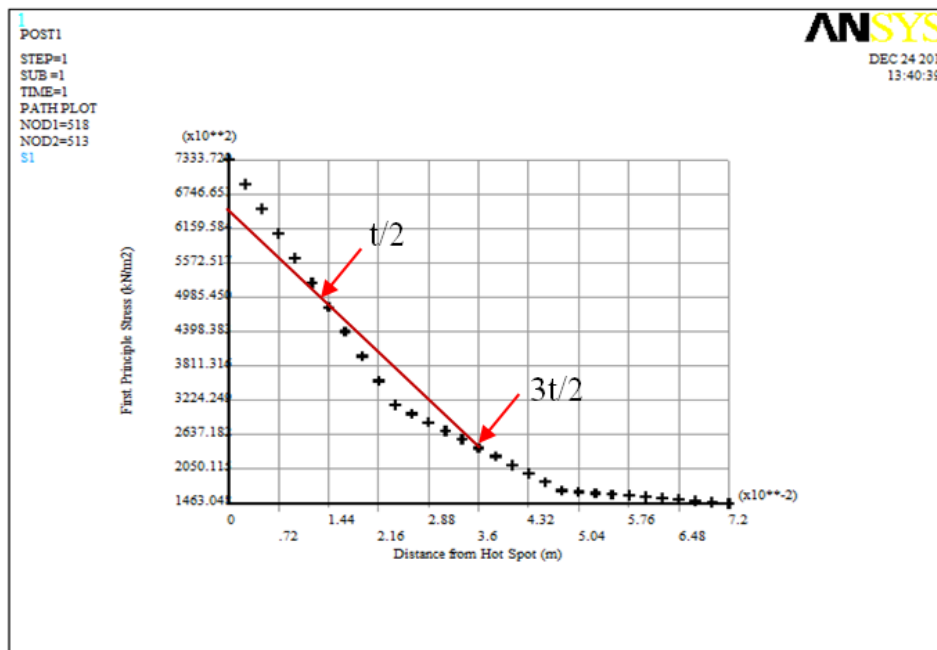


Figure 7-5: First principal stress at nodes

This graph in Figure 7-5 shows the first principal stress at position  $t/2$  and  $3t/2$  from the location of hot spot. Linear extrapolation for the nodal stress at  $t/2$  and  $3t/2$  is formed to

Fatigue strength assessment of a bulk carrier  
according to Common Structural Rules

obtain the hot spot stress. The hot spot value is  $633 \text{ N/mm}^2$ . Comparing the two procedures to evaluate the hot spot stress from nodal points and element center points, there is slightly difference between them. The node stress at hot spot position is equal 1.15 times the extrapolated hot spot value.

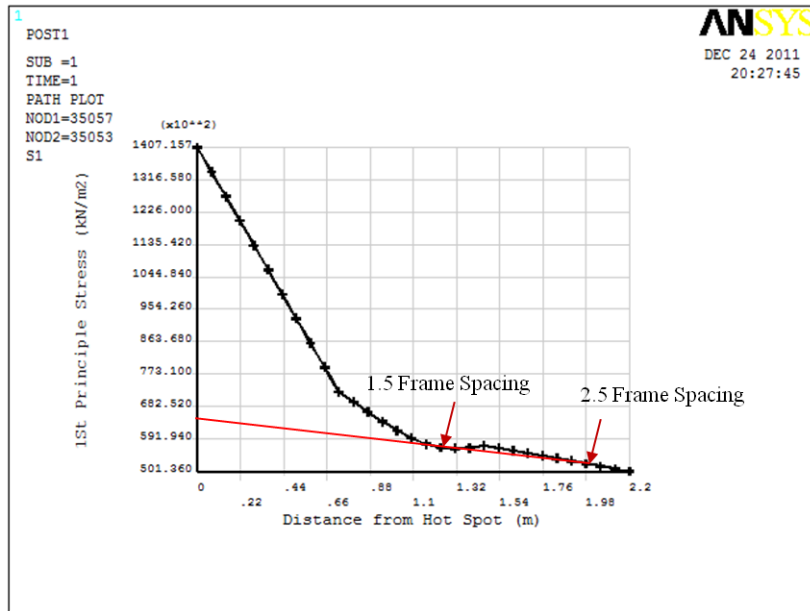


Figure 7-6: First principal stress at nodes from coarse model

The nominal stress at the hot spot location for hopper inner bottom knuckle is determined following the CSR-BC Rules in Chapter 7, Section 4 by extrapolating the first principal stress located at 1.5 times and 2.5 times the frame spacing from the hot spot location, as shown in Figure 7-6. The nominal stress at hot spot site is  $63 \text{ N/mm}^2$ .

The geometry stress concentration factor for hopper inner bottom knuckle is calculated by divided the hot spot stress by the nominal stress at this location, then  $k_g = 633/63 = 10$ .

The geometrical stress concentration factor for hopper inner bottom knuckle can be calculated by the simplified equation in CSR-BC Chapter 7, Section 4, and Subsection 3.3.3 to distinguish with FEM result. The values for the following equations are taken from Table 1 and Table 2 in the previous CSR-BC reference,  $K_{gl} = K_0 K_1$

$K_0$  is stress concentration factor depending on the dimensions of the considered structure and that is founded equal to 3.1 for plate net thickness 22 mm and angle of hopper slope plate to the horizontal  $50^\circ$ .  $K_1$  is correction coefficient depending on the type of knuckle connection

and that is taken 1.7 for weld type. The others coefficients appear in the same equation in CSR-BC taken equal to 1 because there is no insertion of horizontal gusset or longitudinal rib and transverse rib in the created hopper inner bottom knuckle model. Then, the geometry stress concentration factor for the previous detail is equal to 5.27.

Comparing the two estimation value for hopper inner bottom geometry stress concentration factor, one from FEM direct analysis and the other from simplified calculation at IACS Rules, it is found that the factor from FEM approximately double the factor which calculated from the CSR-BC.

### 7.2.2 $K_g$ -Factor for Longitudinal Stiffener Web frame Connection

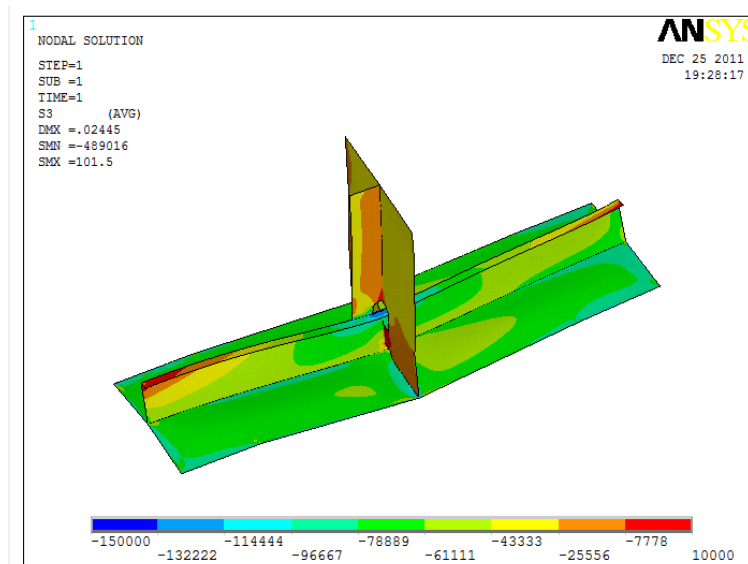


Figure 7-7: Third principal stress distribution in longitudinal-web frame local model

Figure 7-7 shows the hot spot stress in the local submodel of longitudinal-web frame connection after interpolating the displacement from the coarse model with applying internal load for the local model. The Global loading condition applying on that model is alternating load condition when the external hydrodynamic pressure has been maxima. The critical location for the point where the hot spot should be estimated and the expected crack is shown in Figure 7-8

Fatigue strength assessment of a bulk carrier  
according to Common Structural Rules

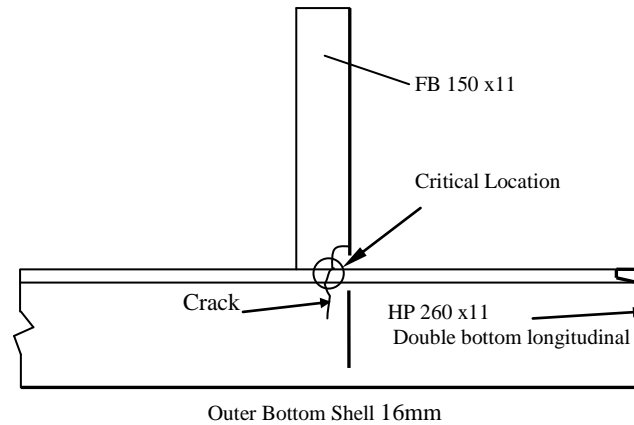


Figure 7-8: Detail in double bottom

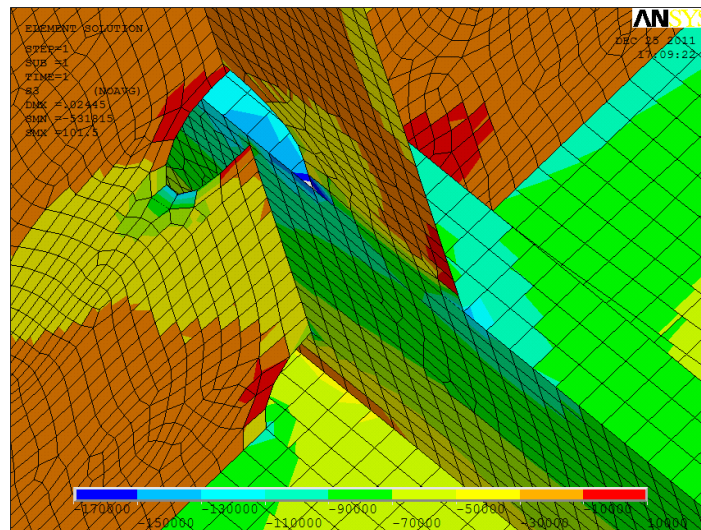


Figure 7-9: Element stress for longitudinal-web frame connection

The third principal element stress distribution around the critical location shows in Figure 7-9. The element center point stress at  $t/2$  and  $3t/2$  where  $t$  the thickness of plate at weld toe from hot spot position is presented in Figure 7-10. The element center point stresses at  $t/2$  and  $3t/2$  are extrapolated to the position of critical detail to estimate the hot spot value. The hot spot stress for longitudinal-web frame end connection value is equal to  $-150.7\text{N/mm}^2$ .

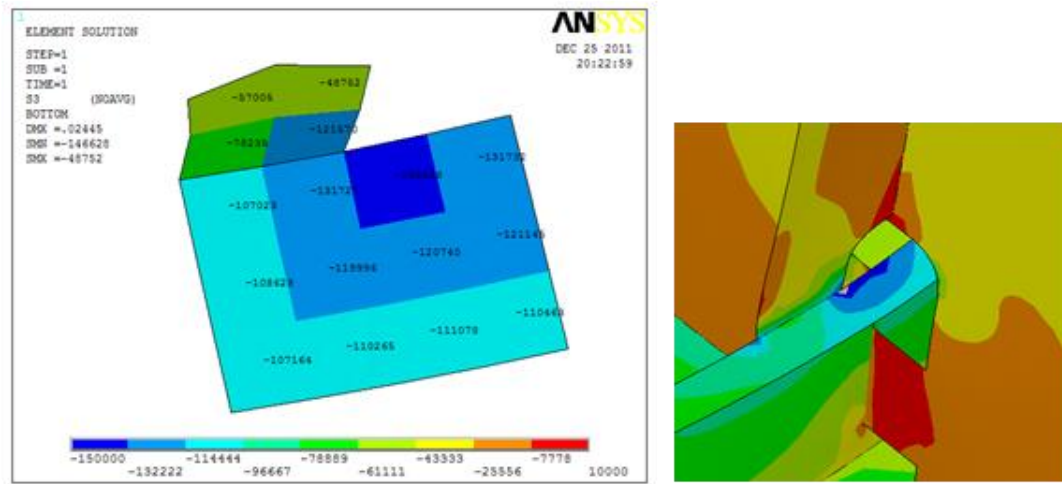


Figure 7-10: Element center point principal stress in longitudinal-web frame model

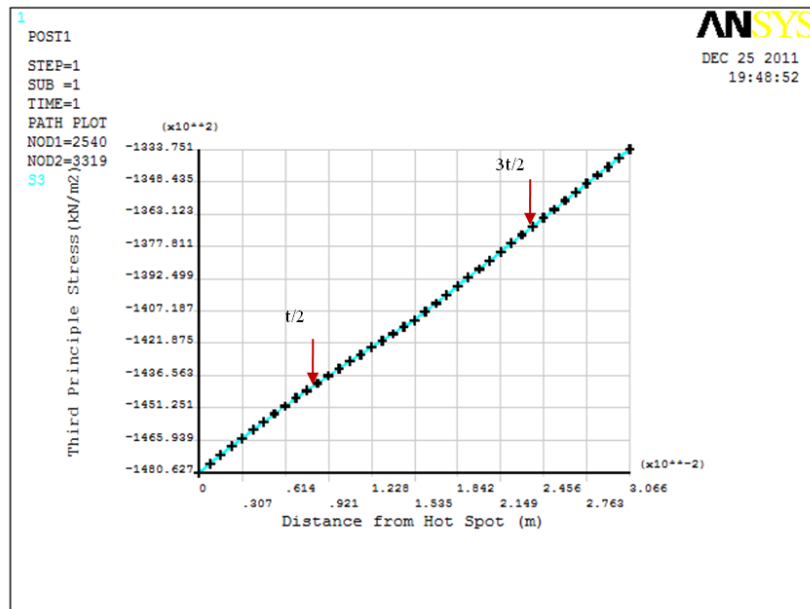


Figure 7-11: Path of hot spot stress for longitudinal-web frame local model

The nodal third principal stress at  $t/2$  and  $3t/2$  from the position of considered hot spot is presented in Figure 7-11. Furthermore, the two previous points are extrapolated to the location of hot spot. The hot spot stress value is  $-148\text{N/mm}^2$ .

The nominal stress is evaluated from the coarse global model in that location as shown in Figure 7-12. Two evaluation procedures will be carried; the first one is extrapolate the element center point stress in longitudinal stiffener web at  $1/2$  frame spacing and  $3/2$  frame spacing to the position of hot spot. The value is founded equal to  $-106\text{N/mm}^2$ . The second one is multiplied the element center point stress in longitudinal stiffener web at  $1/2$  frame spacing by 1.12 and the value is equal to  $-95\text{N/mm}^2$ .



Fatigue strength assessment of a bulk carrier  
according to Common Structural Rules

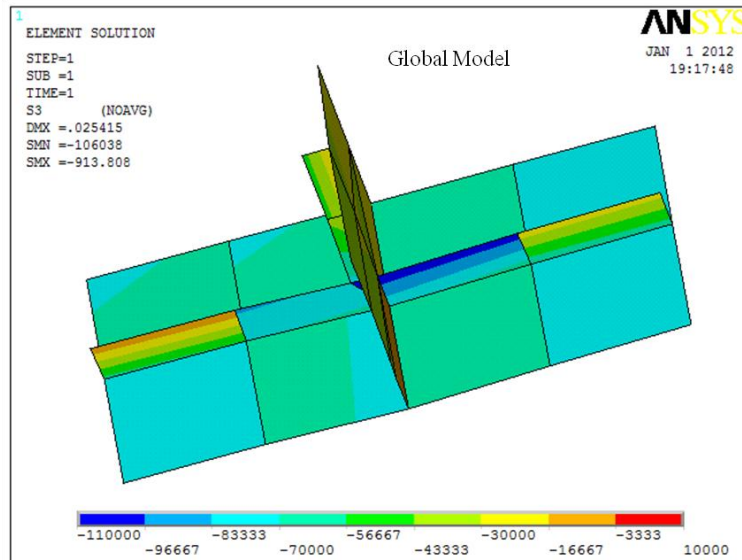


Figure 7-12: Element stress distribution in longitudinal-web frame from global model

The geometry stress concentration factor for longitudinal stiffener web frame connection is calculated from hot spot stress divided by nominal stress. The  $K_g$  value for the considered detail can be 1.58 or 1.42 depends on the evaluated procedure for nominal stress.

CSR-BC has tabulated coefficients in Chapter 8, Section 4 for different geometric structural details to obtain the geometry stress concentration factor. The tables contain two factors: one is geometry stress concentration factor for which the lateral pressure is the only effect and the second is geometry stress concentration factor for the hull girder effect (axial loading). The two  $K_g$  respectively is 1.65 and 1.1 for the same considered geometry of the critical detail and location. Comparing the two values with the one calculated from the direct FEM analysis, it is found that  $K_g$ -factor from FEM is in between the two values obtained from the IACS rules being closer to the larger one. Note, however, that the value obtained from the FEM analysis covers both types of loading while the coefficients in the Rules are given specifically for each loading therefore the results of analysis depends also on the ratio of stresses due to each loading.

Comparing the combined geometry stress concentration factor that obtained from direct FEM analysis for longitudinal-web frame connection with the new tabulated stress concentration factors for top stiffener connection to longitudinal with approximately the same geometry in Classification Notes - No. 34.2, June 2010 Table 8-5. It is found the two factors very close together.

### 7.3. Cumulative Fatigue Damage for Hopper Inner Bottom Knuckle

The fatigue damage assessment for hopper inner bottom knuckle which represent the critical detail in midship cargo hold will be described on the following paragraph. All calculations procedures are reference to CSR-BC Chapter 8, Section 2. The Palmgren-Miner rule of damage accumulation is adopted by IACS Rules and all classification societies. It is state that the cumulative fatigue damage  $D$  calculated for the combined equivalent stress is to be satisfying with the following criteria:

$$D = \sum_i D_j \leq 1.0 \quad (7-1)$$

Where  $D_j$  is elementary fatigue damage for every load condition “ $j$ ”

The cumulative fatigue damage for the  $j$ -th loading conditions is expressed in the CSR-BC as:

$$D_j = \frac{\alpha_j N_L \Delta \sigma_{E,j}^4}{K (\ln N_R)^{4/\xi}} \left[ \Gamma \left( \frac{4}{\xi} + 1, \nu \right) + \nu^{-3/\xi} \gamma \left( \frac{7}{\xi} + 1, \nu \right) \right] \quad (7-2)$$

Where:

$K$ : S-N curve parameter, taken equal to  $1.014 \cdot 10^{15}$

$\alpha_j$ : Coefficient depending on the loading conditions specified in CSR-BC

$N_L$ : Total number of cycles for the design ship's life, taken equal to:

$$N_L = \frac{0.85 T_L}{4 \log L} \quad (7-3)$$

$T_L$ : Design life, in seconds, corresponding to 25 years of ship's life, taken equal to  $7.88 \cdot 10^8$

$L$ : Scantling length of the corresponding bulk carriers and equal 182.3 m.

Then  $N_L$  equal to

$\zeta$ : Weibull shape parameter, taken equal to 1.

$N_R$ : Number of cycles, taken equal to  $10^4$ .

$$\nu = \left( \frac{100.3}{\Delta \sigma_{E,j}} \right)^\xi \ln N_R \quad (7-4)$$

$\Delta \sigma_{E,j}$ : Equivalent notch stress range in  $\text{N/mm}^2$ .

$\Gamma$ : Type 2 or upper non-normalize incomplete gamma function.

$$\Gamma(s, x) = \int_x^\infty t^{s-1} e^{-t} dt \quad (7-5)$$

Where  $x$  is the lower limit of integration and  $s$  is the value of shape parameter

$\gamma$ : Type 1 or lower non-normalize incomplete gamma function.

$$\gamma(s, x) = \int_0^x t^{s-1} e^{-t} dt \quad (7-6)$$

Where  $x$  is the upper limit of integration and  $s$  is the value of shape parameter

The hot spot for the hopper inner bottom knuckle is estimated for each loading conditions considered with the respecting load cases by direct FEM analysis as described in the previous Section 2. The predominant load case ‘I’ among the others is evaluated. The ‘condition 1’ which the maximum stress is calculated by this expression ( $\sigma_{mean,I(k)} + 0.5\Delta\sigma_{W,I(k)}$ ) for the considered member is the largest on the tension side among the loading conditions “homogeneous”, “alternate”, “normal ballast” and “heavy ballast” as shown in Table 7-1.

Table 7-1: Hot spot stress and loading ‘condition 1’

Load condition	Load case	$\sigma_{W,i(k)}$	$\Delta\sigma_{W,i(k)}$	$\sigma_{mean,i(k)}$	$\Delta\sigma_{W,I(k)}$	$\sigma_{mean,I(k)}$	$\sigma_{mean,I(k)} + 0.5\Delta\sigma_{W,I(k)}$	LC #
Homogeneous	1H1	141.70	21.47	152.44	391.2	36.60	232.20	2
	1H2	163.17						
	1F1	292.75	343.19	121.16				
	1F2	-50.44						
	1R1	47.00	193.85	143.93				
	1R2	240.85						
	1P1	-159.00	391.20	36.60				
	1P2	232.20						
Alternate	2H1	-383.00	226.12	-269.94	559.3	-382.35	-102.70	4
	2H2	-156.88						
	2F1	-130.00	334.75	-297.38				
	2F2	-464.75						
	2R1	-426.40	269.00	-291.90				
	2R2	-157.40						
	2P1	-662.00	559.30	-382.35				
	2P2	-102.70						
Normal ballast	3H1	-35.00	54.00	-62.00	334	-193.00	-26.00	3
	3H2	-89.00						
	3F1	-11.00	185.20	-103.60				
	3F2	-196.20						
	3R1	-133.90	81.60	-93.10				
	3R2	-52.30						
	3P1	-360.00	334.00	-193.00				
	3P2	-26.00						
Heavy ballast	4H1	644.75	248.95	520.28	251.49	423.01	548.75	1
	4H2	395.80						
	4F1	548.75	251.49	423.01				
	4F2	297.26						
	4R1	653.11	170.31	567.96				
	4R2	482.80						
	4P1	380.30	32.50	396.55				
	4P2	412.80						

The equivalent notch stress range in  $\text{N/mm}^2$  is calculated as shown in Table 7-2 from the following equation:

$$\Delta\sigma_{eq,j} = K_f f_{mean,j} \Delta\sigma_{W,j} \quad (7-7)$$

The fatigue notch factor  $K_f$  is taken equal to 1.15 from Table 1 in CSR-BC Chapter 8, Section 2 because the considered structure member has full penetration weld. The correction value for mean stress  $f_{mean,j}$  is computed from following Eq. 7-6 and presented in Table 7-2 with taken the residual stress  $\sigma_{res}$  equal to 0 for primary member according to IACS rules. The dominant combined hot spot range  $\Delta\sigma_{W,j}$  is taken from Table 7-1. All equations for the previous calculation have been specified in CSR-BC.

$$f_{mean,j} = \max \left\{ 0.4, \left[ \max \left( 0, \frac{1}{2} + \frac{-\ln(10^{-4})}{4} \frac{\sigma_{m,j}}{\Delta\sigma_{W,j}} \right) \right]^{0.25} \right\} \quad (7-8)$$

The equivalent notch stress range is to be corrected with the following equation:

$$\Delta\sigma_{E,j} = f_{coat} f_{material} f_{thick} \Delta\sigma_{eq,j} \quad (7-9)$$

Correction factor for corrosive environment  $f_{coat}$  is taken equal to 1.05 because hoper inner bottom knuckle structure member is located in cargo hold No. 4 which used for cargo and ballast. Correction factor for material  $f_{material}$  is taken equal to 1 because the minimum yield stress  $R_{eH}$  is  $235\text{N/mm}^2$ . Correction factor for plate thickness  $f_{thick}$  is taken equal to 1.01 because the plate has thickness greater than 22 mm

Table 7-2: Equivalent notch stress ranges

Load condition	LC #	$\sigma_{m,1}$	$\sigma_{mean,1}$	$\sigma_{m,j}$	$f_{mean,j}$	$\Delta\sigma_{eq,j}$	$\Delta\sigma_{E,j}$
Homogenous	2	0	0	-141.11	0.4	179.95	190.01
Alternate	4	0	0	-100.77	0.54	347.44	366.87
Normal ballast	3	0	0	-154.84	0.40	153.64	162.23
Heavy ballast	1	84	423	0.00	1.06	307.03	324.19

The elementary fatigue damage for every load condition “Homogenous”, “Alternate”, “Normal ballast” and “Heavy ballast” is calculated according to Eq. 7-2 as seen in Table 7-3. The corresponding website (<http://danielsooper.com>) has been used to calculate, the non-normalized upper incomplete gamma function  $\Gamma$  and the non-normalized lower incomplete gamma function  $\gamma$  which this website provide statistics calculators.

Table 7-3: Elementary Fatigue damage for hopper inner bottom knuckle

Load condition	$\Delta\sigma_{E,j}$	$\nu$	$\Gamma$	$\gamma$	$\alpha_j$	$D_j$
Homogenous	190.01	4.86	11.1690	600.5870	0.60	0.1304
Alternate	366.87	2.52	21.3230	22.4230	0.10	0.4188
Normal ballast	162.23	5.69	7.8880	1081.3570	0.15	0.0145
Heavy ballast	324.19	2.85	20.1550	45.2370	0.15	0.3727

The cumulative fatigue damage for hopper inner bottom knuckle is computed following Eq. 7-1 and comparing with the damage criteria. It is found that the cumulative damage for the corresponding critical detail for fatigue assessment is equal to 0.936. It is less than one which represents the upper limit for fatigue damage. This means the considered detail can survive up to 25 years in North Atlantic environment without fatigue crack initiation. Figure 7-13 shows that the Alternate loading condition has the highest fatigue damage.

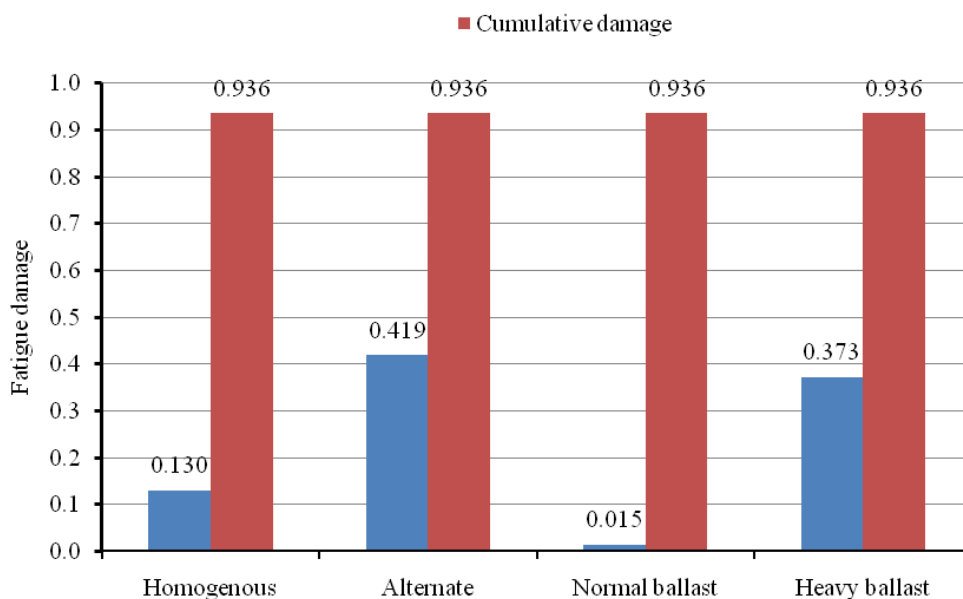


Figure 7-13: Elementary and cumulative fatigue damage for hopper inner bottom knuckle



## 8. CONCLUSIONS AND RECOMMENDATIONS

Coarse FEM model for three midship cargo holds is created using GL Poseidon software for bulk carriers. The global model has been modeled with 4-node shell elements and the model reflects the actual geometry for the relevant DSS bulk carrier. Several matters have been investigated within this work. A lot of effort has been put into modeling and verification of modeling.

Two submodels with fine mesh  $t \times t$  for hopper inner bottom knuckle and longitudinal stiffener web frame connection are developed. Fatigue analysis according to IACS rules using a FE based hot spot stress analysis is carried out. Maximum principal stress in top or/ bottom surface is used for hot stress evaluation and the evaluated stress at the points  $0.5t$  and  $1.5t$  part from hot spot position are extrapolated.

The result of estimation the  $K_g$ -hopper inner bottom knuckle factor shows large differences between compared simplified procedure according to CSR and direct FE analysis. The  $K_g$ -SCF from direct FEM is 10 and 5.27 from simplified method. The combined  $K_g$  factor for longitudinal stiffener web frame from direct FE analysis is 1.58 in between the tabulated factors in CSR-BC 1.64 due lateral pressure effect and 1.1 due hull girder effect.

The  $K_g$  combined factor for longitudinal stiffener web frame end connection depend on the loading effect ratio between lateral pressure (lateral loading) and global hull girder (longitudinal loading). The way to estimate the value of nominal stress from direct FEM analysis has significant effect on the geometry stress concentration factor for both cases.

The extrapolating hot spot stress value from element center points and nodal points at  $t/2$  and  $3t/2$  show slight difference and the two values are very close together.

There is no more detail in a common structure rules for bulk carriers to how extrapolate the hot spot stress and estimate the nominal stress from direct FE analysis.

The cumulative fatigue damage for hopper inner bottom is calculated with considering all loading conditions with respecting load cases. The result show that total fatigue damage for the respecting critical detail is 0.936 less than the limit of cumulative fatigue damage criteria and can survive up to 25 years in North Atlantic environment.

The analysis of hot spot stress ranges for different load conditions is indicate that the highest hot spot stress ranges in homogenous, alternate, normal ballast loading conditions occurred at load case, when the dynamic external pressure is maximum. In addition, for heavy ballast condition occurred in load case when the vertical bending moment is a maximum at following sea condition.

The alternate loading condition and the heavy ballast loading condition respectively have the higher elementary fatigue damage. The local mean stress for heavy ballast load condition 1 has significant influence on the equivalent hot spot stress ranges for all the other loading conditions.

The submodelling is significantly less time consuming nevertheless efficient in getting reasonable result in the region of interest for fatigue analysis. Also, the GL Poseidon software for bulk carrier used as pre-processor for modeling and ANSYS code as post-processor for fatigue analysis is a very efficient way to get good estimation for fatigue assessment.

Finally from that thesis the following further works can be recommended:

Since fatigue accumulation is sensitive to small changes in the predicted hot spot stresses ranges, fatigue investigation should include systematic identifications of error sources in applying design loads and structural modeling and its effect on the predicted fatigue damage. Further finite element analysis using 8-node/or solid elements for the fatigue analysis for these particular details could be done to compare with results from the 4-node shell elements. Also, a simplified procedure to obtain the hot spot stresses can be compared with direct FEM. The different procedures used by the different classification societies in estimation the hot spot stress and the quadratic extrapolation method can be compared in order to found the most suitable result also the same for nominal stress evaluation from direct FE.

Details fatigue analysis using direct FE for hopper inner bottom knuckle submodel with deferent geometry details for all load conditions can be checked to evaluate the geometry stress concentration factors and present it in the rules. The same different longitudinal stiffener web frame end connections geometries can be analyzed for all loading conditions to obtain the combined geometry stress concentration factors and presented as tabulated reference in the rules.



## **9. AKNOWLEGMENTS**

First of all, I am so grateful to my sponsor, Erasmus Mundus EMSHIP programme, for providing this invaluable opportunity to follow my MSc degree at University of Liege, Ecole Centrale de Nantes and West Pomeranian University of Technology, my gratitude also goes to each member of these institutes' staff.

I would like to express my sincere gratitude to my promoter Dr. Maciej Taczala for his thoughtful guidance, unlimited support as well as giving me such precious assistance and feedback throughout the development of my thesis.

I wish to acknowledge the assistance from staff of Genfer Design Company in Szczecin Poland when I am staying in that company for internship to developing my thesis, particularly Dr. Alfred Jazukiewicz and Eng. Piotr Gutowski.

Finally, I would like to express my gratitude to my family, friends, and colleagues for their support and patience.



## 10. REFERENCES

- [1] Yingguang Wang, 2010. *Spectral fatigue analysis of a ship structural detail – A practical case study*, international journal of fatigue, 32, 310-317.
- [2] IACS, 2010. *Common Structural Rules for Bulk Carriers*, Rules for Classification and Construction
- [3] Lovstad, M. and Guttormsen, V. , 2007. *Impact of Common Structural Rules on Software for Ship Design and Strength Assessment*, Proceedings of RINA Int. Conf. on Developments in Classification and International Regulations, London, 119-132.
- [4] Horn, G. and Baumans, P., 2007. *The Development, Implementation and Maintenance of CSR for Bulk Carriers and Oil Tankers*, Proceedings of RINA Int. Conf. On Developments in Classification and International Regulations, London, 25-36.
- [5] American Bureau of Shipping (ABS) , 2010. *Bulk Carrier Solutions: Saver and Stronger Vessels*, Technical Paper.
- [6] Hobbacher, A., 2007, IIW Joint Working Group XIII-XV. 2007. Recommendations for fatigue design of welded joints and components. IIW document XIII-2151-07 / XV-1254-07, Paris, France, 2007.
- [7] ISSC Committee III.2, 2009. *Fatigue and Fracture Report*, The 117th International Ship And Offshore Structures Congress, 16-21 August 2009, Seoul, Korea.
- [8] Sharp, J.V., 1993. *Effect of Uncertainties in Predicted Fatigue Life on Structural Reliability, Integrity of Offshore Structures*, EMAS Scientific Publications. 5, 215-234.
- [9] Poutiainen, I., Tanskanen, P. and Marquis, G., 2004. *Finite Element Methods for Structural Hot Spot Stress Determination – a Comparison of Procedures*. International Journal of Fatigue, Vol. 26, 1147-1157.
- [10] Lotsberg, I., 2006a. *Fatigue Design of Plated Structures using Finite Element Analysis*, Ships and Offshore Structures, 1:1, 45-54.
- [11] Lotsberg, I., 2007. *Recent Advances on Fatigue Limit State Design for FPSOs*, Ships and Offshore Structures, 2:1, 49-68.
- [12] Lotsberg, I., 2006b. *Assessment of Fatigue Capacity in the new Bulk Carrier and Tanker Rules*, Marine Structures, 20:1-2, 83-96.
- [13] IACS, 1999. *Fatigue Strength of Ship Structures*, Recommendation Note, No. 56.
- [14] <http://danielsoper.com> [Accessed 1 January 2012].
- [15] DNV, 2010a. *Fatigue Assessment of Ship Structures*, Classification Notes, No. 30.7.
- [16] DNV, 2010b. *Plus-Extended Fatigue Analysis of Ship Details*, Classification Notes, No. 34.2.
- [17] Germanischer Lloyd SE, 2011. *CSR-BC POSEIDON User Manual*.
- [18] ANSYS, 2009. *Help User Manual*.
- [19] Mitsuru K., et al., 2002. *Submodelling Analysis of Ship Structure with Super Convergent Patch Recovery Method*, Proceedings of the Twelfth International Offshore and Polar Engineering Conference, Kitakyushu, Japan, May 26-31.
- [20] SSC, 1999. *Fatigue Resistant detail design guide for Ship Structures*, SSC-405



## APPENDICES

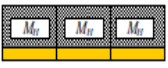




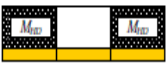


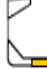











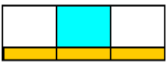




### Appendix A1: Load Combination Factors

Table 3: Load combination factors LCF

	LCF	H1	H2	F1	F2	R1	R2	P1	P2
$M_{WV}$	$C_{WV}$	-1	1	-1	1	0	0	$0.4 - \frac{T_{IC}}{T_S}$	$\frac{T_{IC}}{T_S} - 0.4$
$Q_{WV}$	$C_{QW}^{(1)}$	-1	1	-1	1	0	0	$0.4 - \frac{T_{IC}}{T_S}$	$\frac{T_{IC}}{T_S} - 0.4$
$M_{WH}$	$C_{WH}$	0	0	0	0	$1.2 - \frac{T_{IC}}{T_S}$	$\frac{T_{IC}}{T_S} - 1.2$	0	0
$a_{surge}$	$C_{XS}$	-0.8	0.8	0	0	0	0	0	0
$a_{pitch x}$	$C_{XP}$	1	-1	0	0	0	0	0	0
$g \sin \Phi$	$C_{XG}$	1	-1	0	0	0	0	0	0
$a_{sway}$	$C_{YS}$	0	0	0	0	0	0	1	-1
$a_{roll y}$	$C_{YR}$	0	0	0	0	1	-1	0.3	-0.3
$g \sin \theta$	$C_{YG}$	0	0	0	0	1	-1	0.3	-0.3
$a_{heave}$	$C_{ZH}$	$0.6 \frac{T_{IC}}{T_S}$	$-0.6 \frac{T_{IC}}{T_S}$	0	0	$\frac{\sqrt{L}}{40}$	$-\frac{\sqrt{L}}{40}$	1	-1
$a_{roll z}$	$C_{ZR}$	0	0	0	0	1	-1	0.3	-0.3
$a_{pitch z}$	$C_{ZP}$	1	-1	0	0	0	0	0	0
(1) The LCF for $C_{QW}$ is only used for the aft part of midship section. The inverse value of it should be used for the forward part of the midship section.									

## Appendix A2: Standard Loading Condition for Fatigue Assessment

Table 1: Fatigue Assessment applicable to empty hold in alternate condition of BC-A (mid-hold is empty hold)

No.	Description	Draught <sup>a)</sup>	Loading pattern	Aft	Mid	Fore	Load case (Design wave)				Still water vertical bending moment <sup>b)</sup>	Remarks (see below)		
							H1	F1	R1	P1				
1	Full Load	$T$						H1	F1	R1	P1	$M_{S,(1)}$	1)	
								H2	F2	R2	P2			
2	Alternate Load	$T$						H1	F1	R1	P1	$M_{S,(2)}$	2)	
								H2	F2	R2	P2			
3	Normal Ballast	$T_{NB}$						H1	F1	R1	P1	$M_{S,(3)}$		
								H2	F2	R2	P2			
4	Heavy Ballast	$T_{HB}$						H1	F1	R1	P1	$M_{S,(4)}$	3)	
								H2	F2	R2	P2			
									H1	F1	R1	P1	$M_{S,(4)}$	4)
									H2	F2	R2	P2		

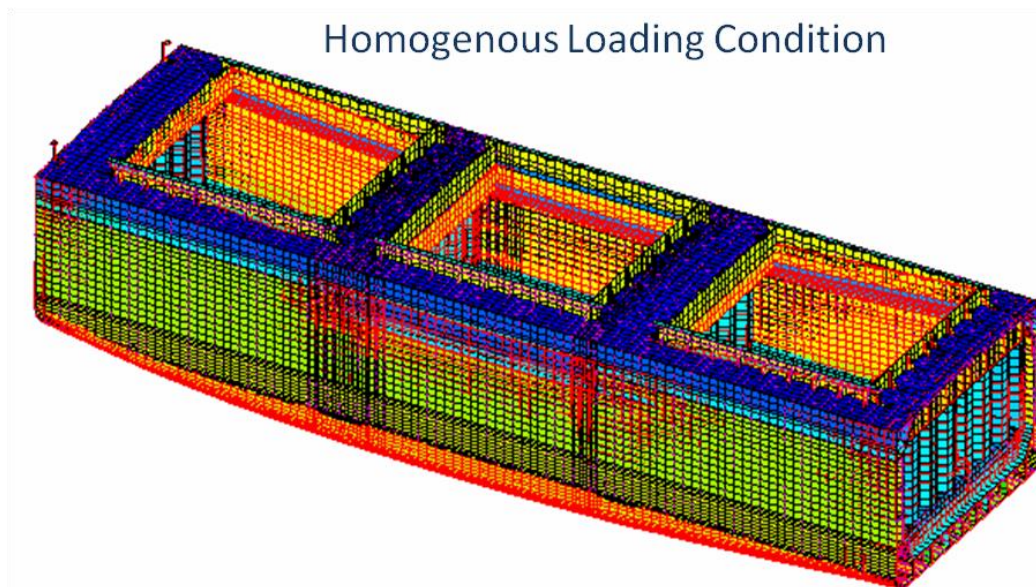
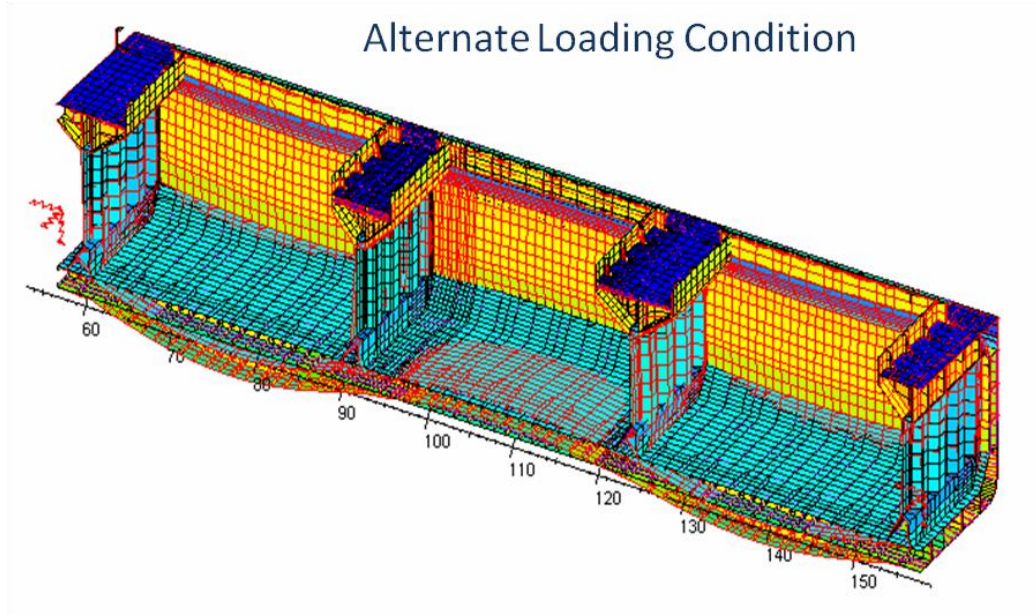
a)  $T$ : Moulded draught,  $T_{NB}$ : Draught at normal ballast condition,  $T_{HB}$ : Draught at heavy ballast condition

b)  $M_{S,(1)}, M_{S,(2)}, M_{S,(3)}, M_{S,(4)}$ : Still water vertical bending moment as defined in [3.2.2] of Ch 8, Sec 3

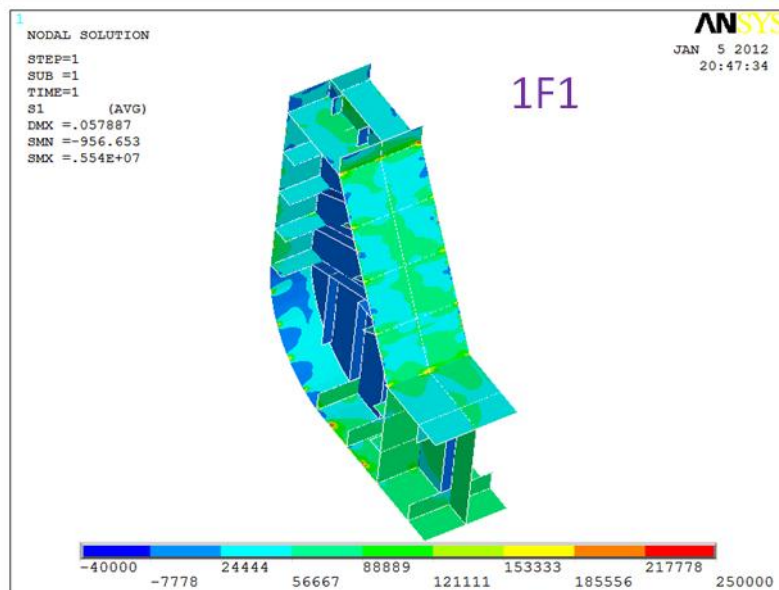
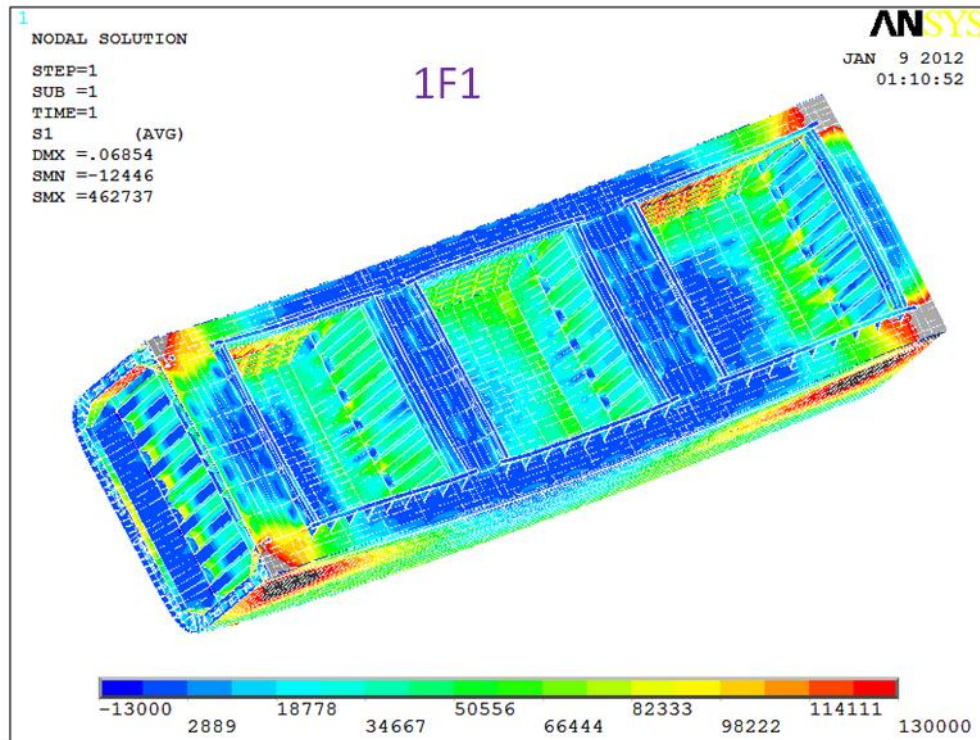
## Remarks

- 1)  $M_H/V_H$  is to be used as cargo density for calculation of dry cargo pressure.
- 2) Cargo density  $3.0 \text{ t/m}^3$  is to be used for calculation of dry cargo pressure in principle.
- 3) This condition is to be applied only for the empty hold which is not assigned as ballast hold. Position of ballast hold is to be adjusted as appropriate.
- 4) This condition is to be applied only for the empty hold which is assigned as ballast hold.

Appendix A3: Deformation in Global Coarse Model (Poseidon Code)



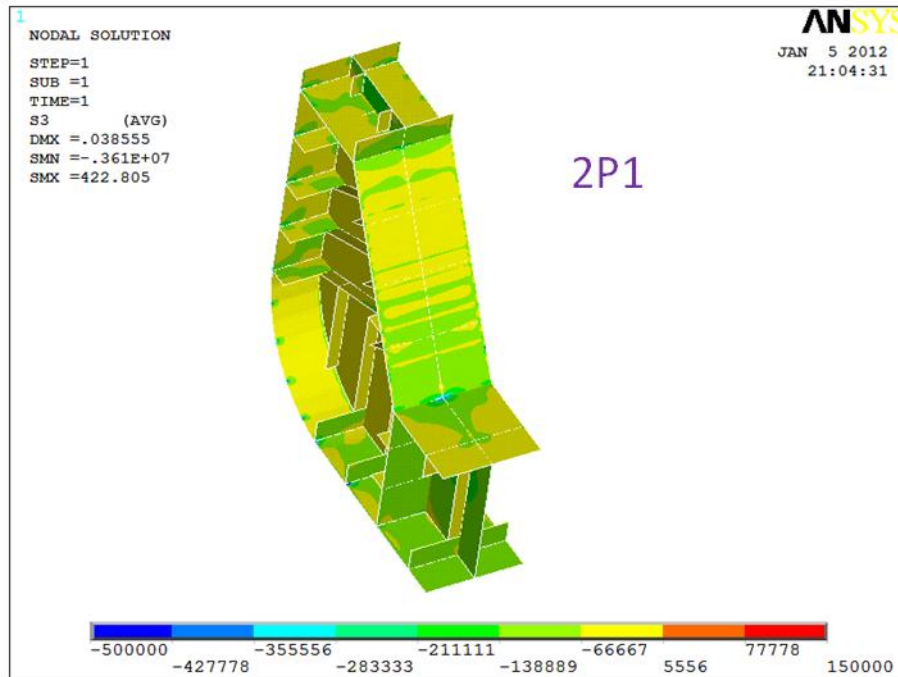
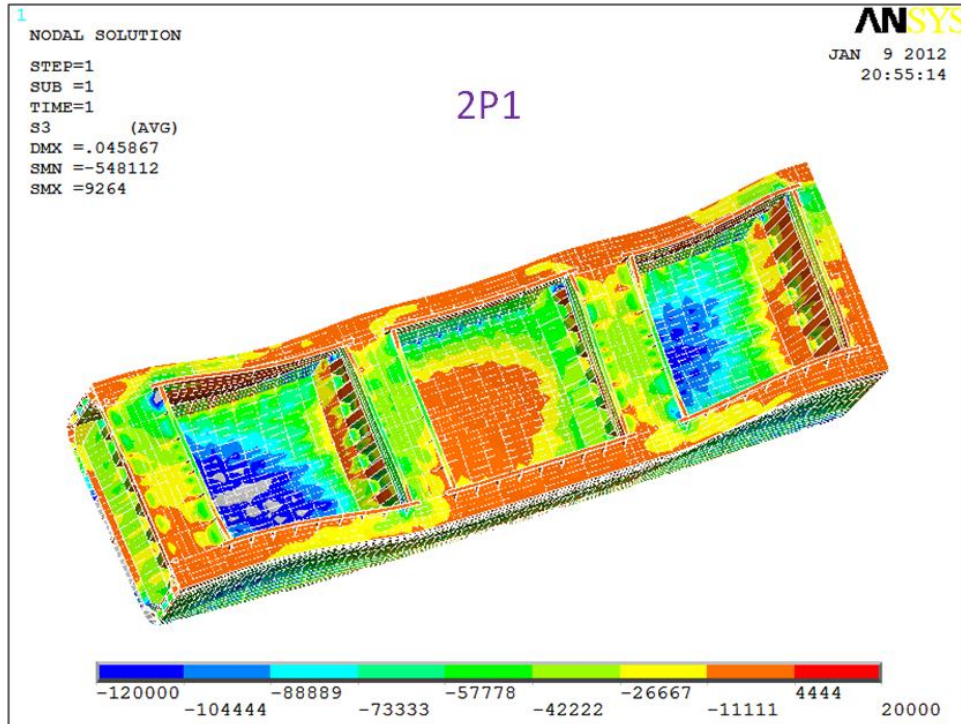
Appendix A4: Principal Stress in Coarse Model and Submodel for Homogenous Loading Condition



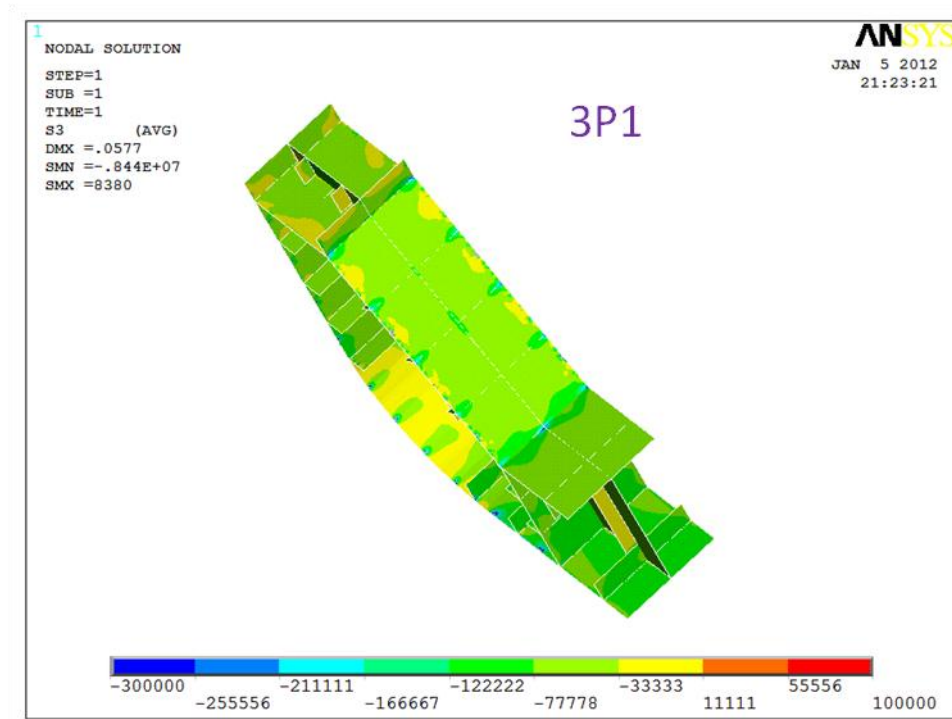
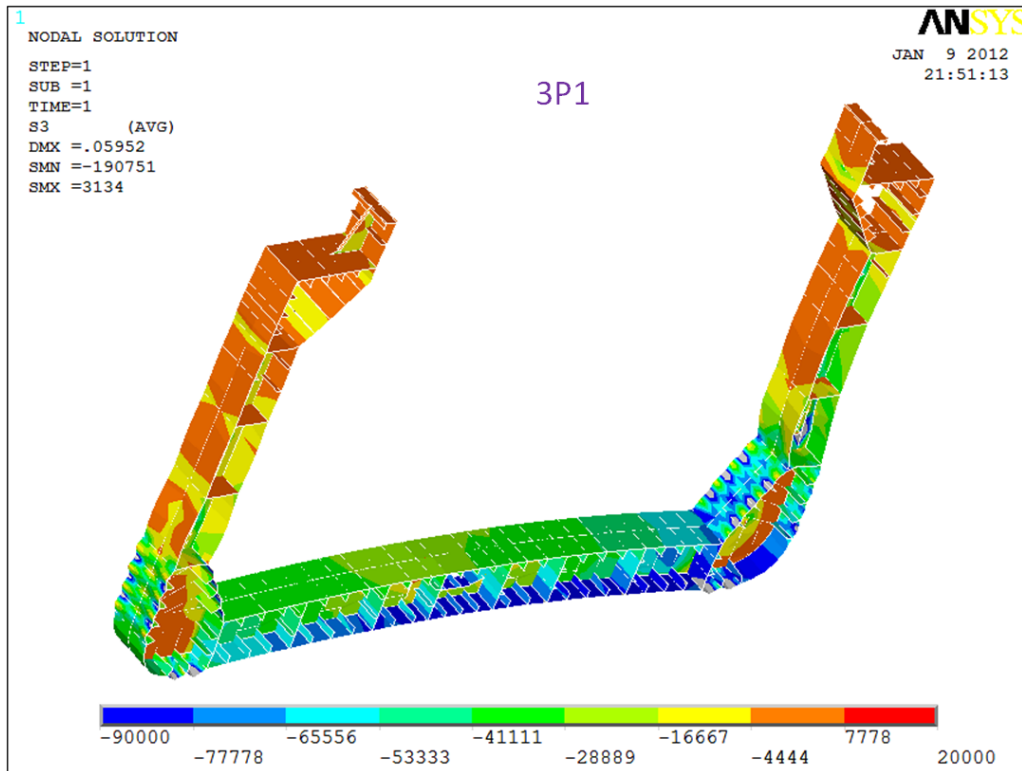


Fatigue strength assessment of a bulk carrier  
according to Common Structural Rules

Appendix A5: Principal Stress in Coarse Model and Submodel for Alternate Loading Condition

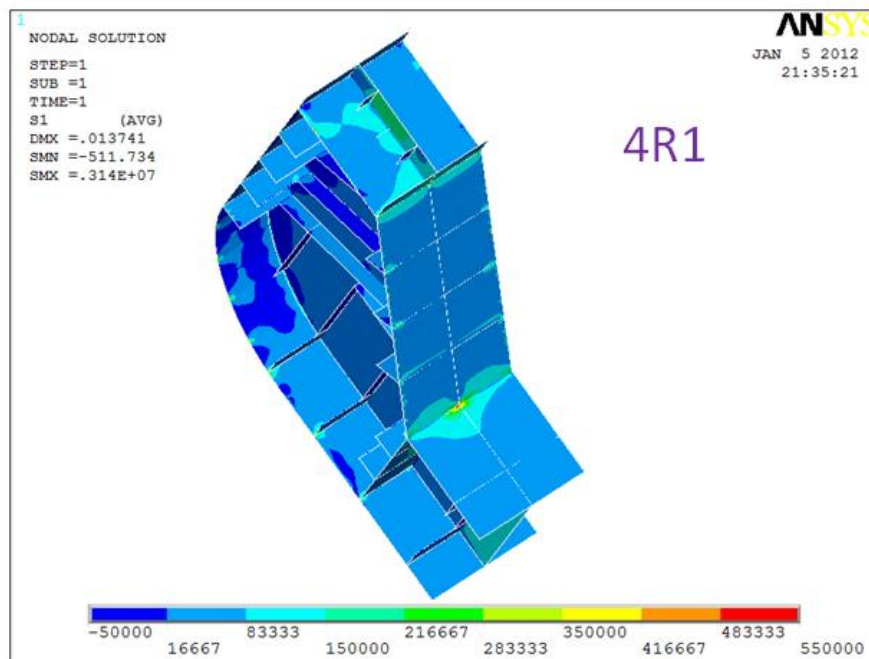
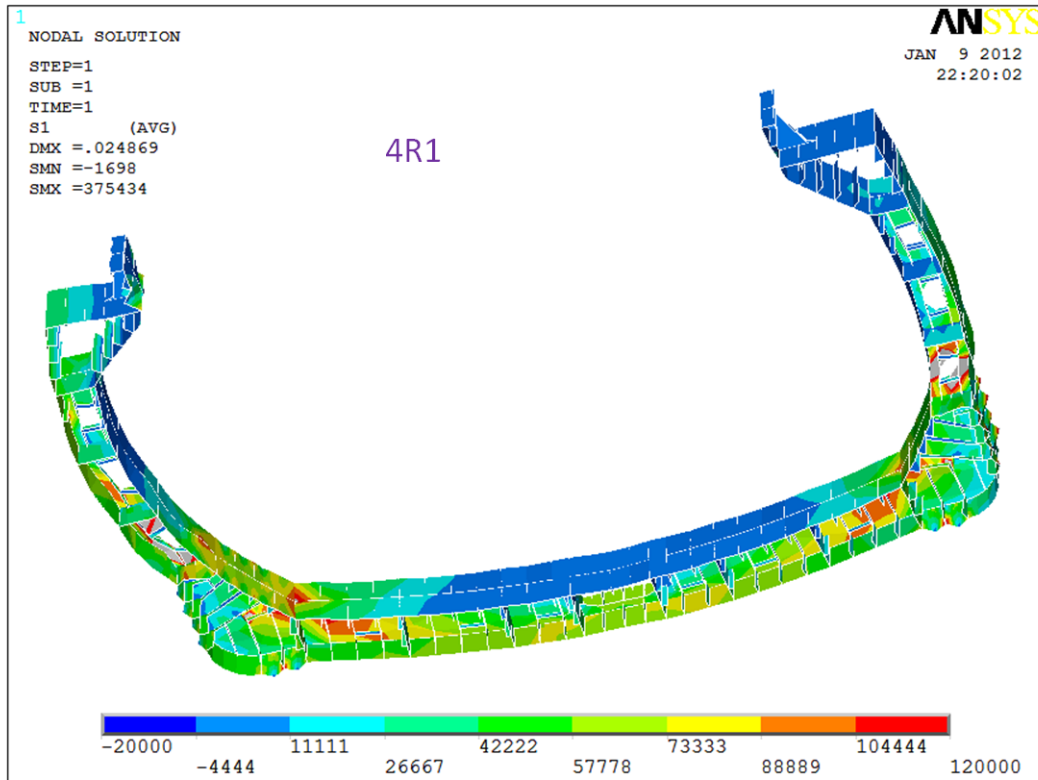


Appendix A6: Principal Stress in Coarse Model and Submodel for Normal Ballast Loading Condition

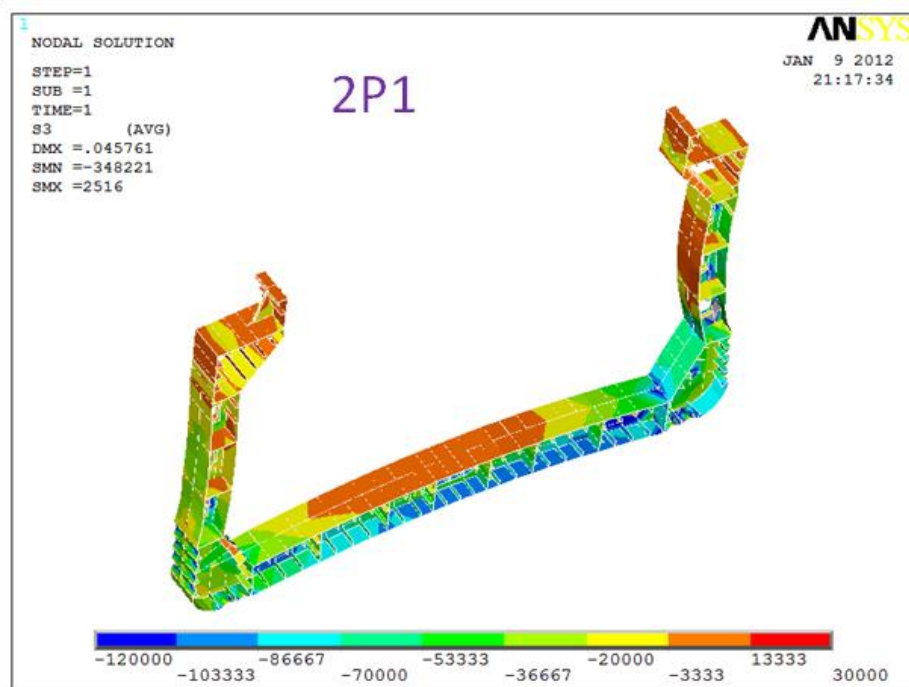
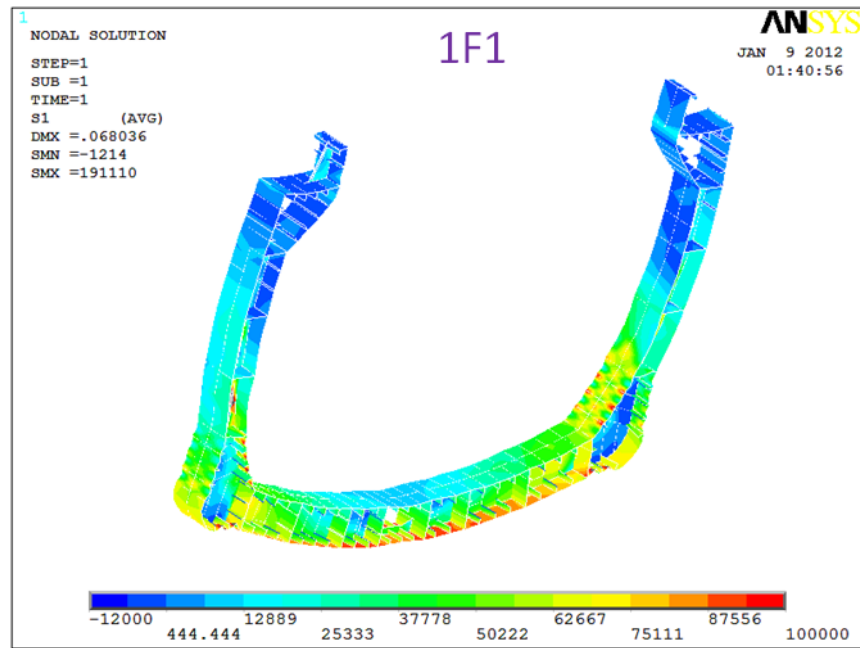


Fatigue strength assessment of a bulk carrier  
according to Common Structural Rules

Appendix A7: Principal Stress in Coarse Model and Submodel Heavy Ballast Loading Condition

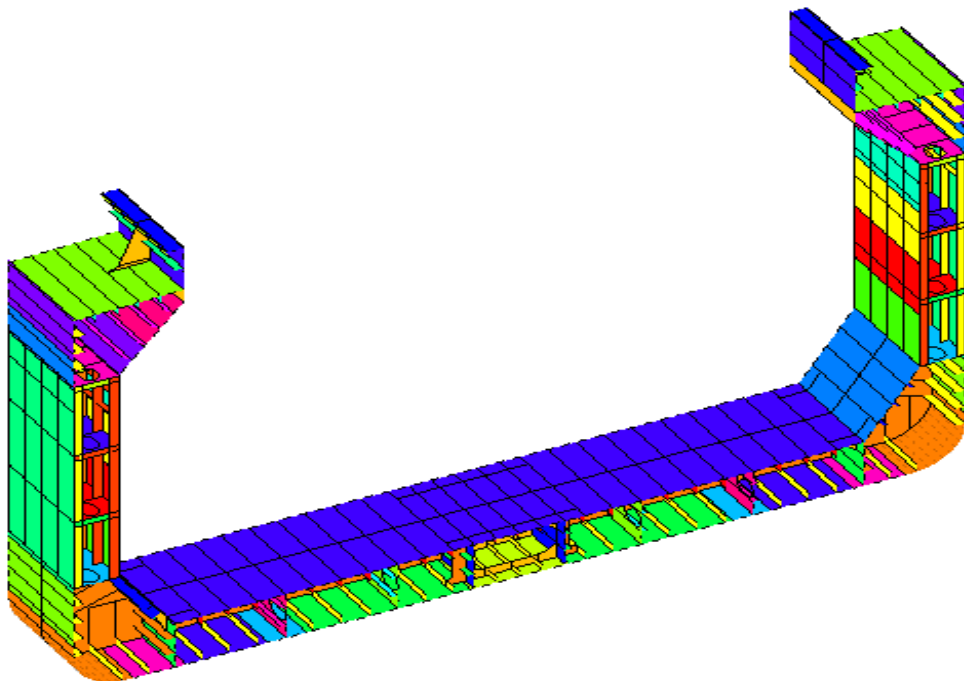
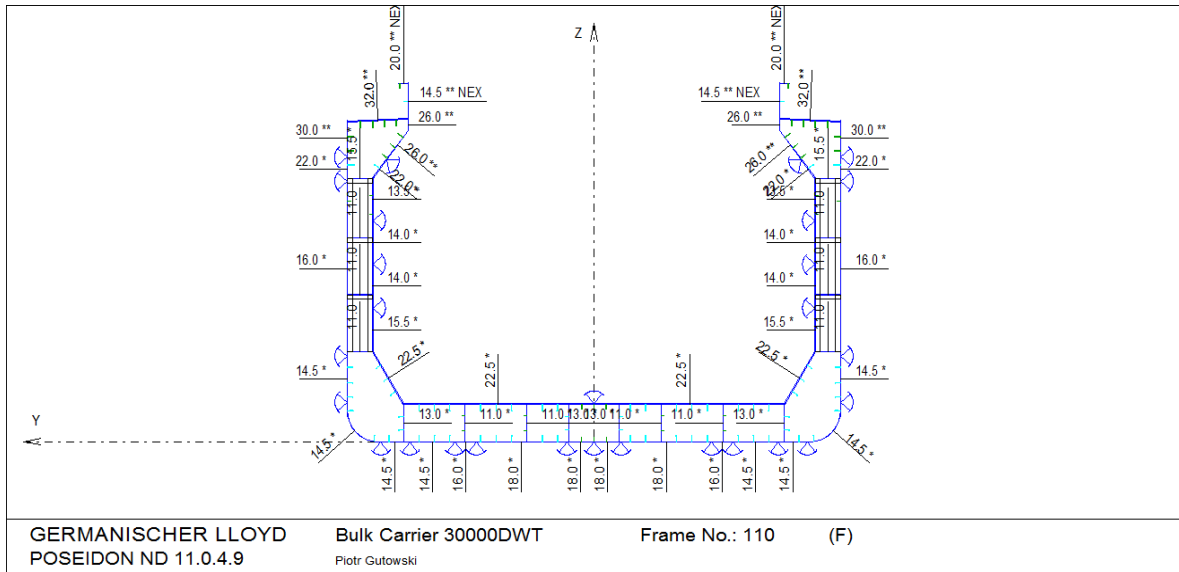


Appendix A8: Principal Stress in Coarse Model Homogenous and Alternate Load Conditions

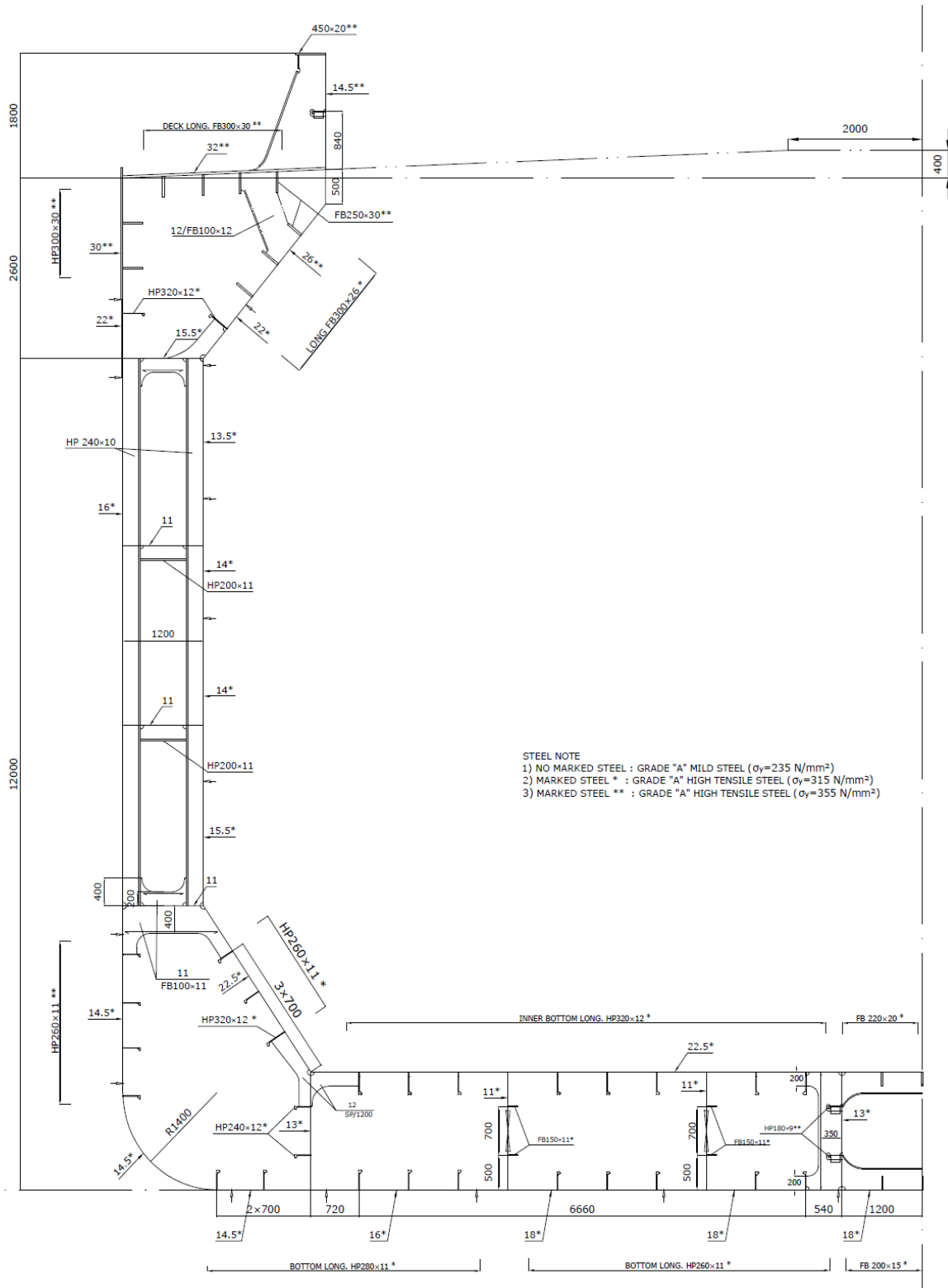


Fatigue strength assessment of a bulk carrier  
according to Common Structural Rules

Appendix A9: Midship Section of DSS Bulk Carrier (Poseidon Code)



Appendix A10: Ordinary Frame Midship Section in Cargo Hold



Fatigue strength assessment of a bulk carrier according to Common Structural Rules

Appendix A11: Path of nodal principal stress for different loading conditions from hot spot

